Error Rate and Power Allocation Analysis of Regenerative Networks Over Generalized Fading Channels

Mulugeta K. Fikadu, *Student Member, IEEE*, Paschalis C. Sofotasios, *Member, IEEE*, Sami Muhaidat, *Senior Member, IEEE*, Qimei Cui, *Senior Member, IEEE*, George K. Karagiannidis, *Fellow, IEEE*, and Mikko Valkama, *Senior Member, IEEE*

***Abstract*—Cooperative communication has been shown to provide significant increase of transmission reliability and network capacity while expanding coverage in cellular networks. The present work is devoted to the investigation of the end-to-end performance and power allocation of a maximum-ratio-combining based regenerative multi-relay cooperative network over non-homogeneous scattering environment, which is the realistic case in many practical wireless communication scenarios. Novel analytic expressions are derived for the end-to-end symbol-error-rate of both M-ary phase-shift keying and M-ary quadrature amplitude modulation over independent and non-identically distributed generalized fading channels are given by exact analytic expressions that involve the Lauricella function and can be readily evaluated with the aid of a proposed computing algorithm. Simple analytic expressions are also derived for the corresponding symbol-error-rate at asymptotically high signal-to-noise ratios. The derived expressions are corroborated with respective results from computer simulations and are subsequently employed in formulating a sum-power optimization problem that enhances the system performance under total sum-power constraint within the multi-relay cooperative system. It is also shown that asymptotically optimum power allocation provides substantial performance gains over the corresponding equal power allocation, particularly, when the source-relay and relay-destination paths are highly unbalanced.**

***Index Terms*—Cooperative communications, asymptotic analysis, decode-and-forward, digital modulations, fading channels, special functions, maximum-ratio-combining, relay systems, power allocation.**

Manuscript received June 7, 2015; revised November 21, 2015; accepted December 28, 2015. Date of publication January 12, 2016; date of current version April 13, 2016. This work was supported by the Finnish Funding Agency for Technology and Innovation (Tekes) under the project entitled "Energy-Efficient Wireless Networks and Connectivity of Devices-Systems (EWINE-S)", by the Academy of Finland under the projects No. 284694 and No. 288670 and by the National Nature Science Foundation of China Project "Grant No. 61471058." This paper was presented in part at the 10th IEEE WiMob '14, Larnaca, Cyprus and at the 11th IEEE WiMob '15, Abu Dhabi, United Arab Emirates. The associate editor coordinating the review of this paper and approving it for publication was H.-C. Yang.

M. K. Fikadu and M. Valkama are with the Department of Electronics and Communications Engineering, Tampere University of Technology, Tampere 33101, Finland (e-mail: mulugeta.fikadu@tut.fi; mikko.e.valkama@tut.fi).

P. C. Sofotasios is with the Department of Electronics and Communications Engineering, Tampere University of Technology, Tampere 33101, Finland, and also with the Department of Electrical and Computer Engineering, Aristotle University of Thessaloniki, Thessaloniki 54124, Greece (e-mail: p.sofotasios@ieee.org).

S. Muhaidat is with the Department of Electrical and Computer Engineering, Khalifa University, Abu Dhabi, UAE, and also with the Department of Electronic Engineering, University of Surrey, Guildford GU2 7XH, U.K. (e-mail: muhaidat@ieee.org).

Q. Cui is with the School of Information and Communication Engineering, Beijing University of Posts and Telecommunications, Beijing 100876, China (e-mail: cuiqimei@bupt.edu.cn).

G. K. Karagiannidis is with the Provincial Key Lab of Information Coding and Transmission, Southwest Jiaotong University and with the Electrical and Computer Engineering Department, Aristotle University of Thessaloniki, Thessaloniki GR-54124, Greece (e-mail: geokarag@auth.gr).

Color versions of one or more of the figures in this paper are available online at http://ieeexplore.ieee.org.

Digital Object Identifier 10.1109/TCOMM.2016.2517143

I. Introduction

Cooperative transmission methods have attracted significant interest over the past decade due to their applicability in size, power, hardware and price constrained devices such as cellular mobile devices, wireless sensors, ad-hoc networks and military communications [1]–[10]. Such systems exploit the broadcast nature and the inherent spatial diversity of wireless paths and are typically distinguished between regenerative (decode-and-forward) or non-regenerative (amplify-and-forward) relaying schemes. The digital processing nature of regenerative relaying is considered more efficient than non-regenerative relaying, as the latter typically requires costly RF transceivers in order to avoid forwarding a noisy version of the signal [11]–[17].

The performance of cooperative systems can be substantially improved by optimum allocation of the limited overall power to the source and relays of the network in order to minimize the overall energy consumption for given end-to-end performance specifications. Among others, this can be efficiently achieved by accurately accounting for the detrimental effects of multipath fading. Based on this, the authors in [18] derived upper and lower bounds for the outage probability (OP) of multi-relay decode-and-forward (DF) networks over independent but non-identically distributed (i.n.i.d) Nakagami$-m$ fading channels. In the same context, the authors in [19] analyzed the symbol error rate (SER) and OP of DF systems with relay selection over i.n.i.d Nakagami$-m$ fading channels, with integer values of m, whereas a comprehensive analytical framework for a multi-antenna DF system under multipath fading was derived in [20]. Likewise, the performance of DF systems over different fading environments was investigated in [21]–[25], whereas analysis for the SER of DF relaying for M-ary phase-shift keying ($M-$PSK) and M-ary quadrature amplitude modulation ($M-$QAM) over Nakagami$-m$ fading channels was reported in [26]. In addition, the optimum power allocation (OPA) in regenerative relaying with respect to pre-defined thresholds for the SER and OP was analyzed in [26] and [27], respectively. This problem was also addressed in [28] and [29] for multi-node DF relaying based on asymptotic SER and for a given network topology over Rayleigh fading channels, respectively. In the same context, the authors in [30] proposed power allocation schemes for the case of multi-relay DF communications in the high-SNR regime over Nakagami$-m$ fading channels.

Nevertheless, all reported investigations addressing the performance and OPA for resource constrained cooperative networks have been focusing on the case of Rayleigh or Nakagami$-m$ multipath fading conditions. However, it is recalled that these fading models are based on the underlying concept of homogeneous scattering environments, which is not necessarily technically realistic because surfaces in most radio propagation environments are in practice spatially correlated [31]–[42], and the references therein. This issue was addressed in [32] by proposing the $\eta-\mu$ distribution, which is a generalized fading model that has been shown to provide particularly accurate fitting to realistic measurement results, while it includes as special cases the well known Rayleigh, Nakagami$-m$ and Hoyt distributions [31]–[33] and [43]–[48]. Based on this, several contributions have been devoted to the analysis of various communication scenarios over generalized fading channels that follow the $\eta-\mu$ distribution, see, e.g., [44]–[50] and the references therein. Motivated by this, the present work is devoted to the evaluation of the end-to-end SER in regenerative cooperative communication systems with multiple relays for $M-$PSK and $M-$QAM constellations over generalized fading channels and to the corresponding power allocation optimization. Specifically, the contributions of this work are summarized below:

- Exact analytic expressions are derived for the end-to-end SER of $M-$PSK and $M-$QAM based multi-relay regenerative networks over generalized multipath fading environments for both i.n.i.d and i.i.d scenarios using maximum-ratio-combining (MRC) at the destination.
- Simple asymptotic expressions are derived for the above scenarios for high SNR values.
- The corresponding amount of fading is derived for quantifying the respective fading severity.
- Optimal power allocation based on the convexity of the derived asymptotic expressions is formulated, to minimize the corresponding SER under sum-power constraint in all nodes.
- The derived expressions are employed in evaluating the performance of the considered system, which leads to the extraction of useful insights.
- It is shown that a 3dB gain is achieved by the determined OPA even for a small number of relays.
- It is shown that post-Rayleigh fading conditions result to an improved performance by up to 4dB compared to communications over severe multipath fading conditions.
- It is shown that a maximum gain of about 21dB occurs, compared to ordinary direct communication, even if only few nodes are employed in non-severe fading conditions. This renders the resource constrained communication system a meaningful alternative for increasing the quality of service of demanding emerging wireless systems.
- A simple MATLAB algorithm is proposed for the computation of the generalized Lauricella function.

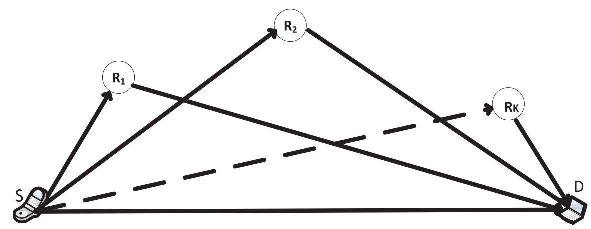

Fig. 1. Multi-node dual hop cooperative relay system.

The remainder of the paper is organized as follows: Section II revisits the considered system and channel models. The exact and asymptotic SER expressions for $M-$QAM and $M-$PSK constellations over generalized multipath fading channels are derived in Section III. The asymptotically optimum power allocation scheme based on sum-power constraint is provided in Section IV while Section V presents the corresponding numerical results along with related discussions and insights. Finally, closing remarks are given in Section VI.

II. System and Channel Models

A. System Model

We consider a multi-node cooperative radio access system consisting of a source node S, intermediate relay nodes R_k, with $k = \{1, 2, \cdots, K\}$, and a destination node D, as depicted in Fig. 1. Each node in the system is equipped with a single antenna while a half-duplex decode-and-forward protocol is adopted. Furthermore, it is assumed that the transmission channels for all relays are orthogonal, such that the transmitted signals from each relay can be separately processed at the destination without any interference from other relays, and finally combined in order to obtain the corresponding cooperation gain. A most common approach to compose such orthogonal channels is the time-based model, where $K + 1$ different time slots are adopted and allocated properly. In this case, the first slot is used for broadcasting from the source to the destination and to all K relays, while the following K slots are subsequently used, one relay at a time, to transmit re-encoded and modulated signals from relays to the destination, as in [10], [27], [28], [30]. Alternative effective approaches can be obtained through frequency division multiplexing (FDM) and code division multiplexing (CDM), primarily orthogonal frequency division multiple-access (OFDMA) and code division multiple access (CDMA). In the OFDMA scenario, $K + 1$ different subsets or sub-bands of subcarriers can provide the orthogonal channels while in the CDMA case, this can be realized by $K + 1$ different orthogonal spreading codes[1]. Based on

[1] In the present work, we do not explicitly assume any of the above models but instead emphasize on the availability of the orthogonal resources, which ensure that the inter-relay interference at the destination node is ultimately avoided.

this and without loss of generality, the received signals in the first time slot can be represented as follows:

$$y_{S,D} = \sqrt{P_0}\alpha_{S,D}x + n_{S,D} \tag{1}$$

and

$$y_{S,R_k} = \sqrt{P_0}\alpha_{S,R_k}x + n_{S,R_k} \tag{2}$$

where P_0 is the source transmit power, x is the transmitted symbol with normalized unit energy in the first transmission phase, $\alpha_{S,D}$ and α_{S,R_k} are the complex fading coefficients from the source to the destination and from the source to the k^{th} relay, respectively, whereas $n_{S,D}$ and n_{S,R_k} represent the corresponding additive-white-Gaussian noise (AWGN) with zero mean and variance N_0. In the next time slot(s), depending on the adopted strategy, if the k^{th} relay decodes correctly, it forwards the decoded and re-encoded signal to the destination over the k^{th} orthogonal channel with power P_{R_k}; otherwise, it remains silent. To this effect, the received signal at the destination can be expressed as follows:

$$y_{R_k,D} = \sqrt{C(k)P_{R_k}}\alpha_{R_k,D}x + n_{R_k,D} \tag{3}$$

where $C(k) = 1$ if the k^{th} relay decodes successfully and $C(k) = 0$, otherwise. Also, $\alpha_{R_k,D}$ denotes the complex fading coefficient from the k^{th} relay to the destination and $n_{R_k,D}$ is the corresponding AWGN. It is also assumed that each path experiences narrowband multipath fading that follows the $\eta - \mu$ distribution and that MRC diversity is employed at the destination. Based on this, the corresponding combined output received signal can be expressed as follows:

$$y_D = w_0 y_{S,D} + \sum_{k=1}^{K} w_k y_{R_k,D} \tag{4}$$

where

$$w_0 = \frac{\sqrt{P_0}\alpha^*_{S,D}}{N_0} \tag{5}$$

and

$$w_k = \frac{\sqrt{C(k)P_{R_k}}\alpha^*_{R_k,D}}{N_0} \tag{6}$$

denote the optimal MRC coefficients for $y_{S,D}$ and $y_{R_k,D}$, respectively with $(\cdot)^*$ representing the complex conjugate operator.

It is noted that in any considered strategy of assigning orthogonal channels, if the mapping of the physical resources i.e. time slots, frequencies, or codes is practically fixed and a particular relay node fails to decode correctly, the corresponding physical resource is momentarily left unused. On the other hand, if a centralized but dynamic resource management is available in the system, the physical resources can be allocated or re-allocated dynamically for e.g. always to those nodes that are able to decode correctly. This, however, requires additional control signaling between the relay nodes and the central control unit, which in turn reduces relatively the efficiency of the overall resource use on its own[2].

[2]These aspects are not addressed further in this article, but they form an important topic for our future work.

TABLE I
RELATION BETWEEN $\eta-\mu$ DISTRIBUTION AND OTHER COMMON FADING DISTRIBUTIONS

Fading Distribution	Format-1	Format-2
$\eta - \mu$	$h = (2+\eta^{-1}+\eta)/4,\ H = (\eta^{-1}-\eta)/4$	$h = 1/(1-\eta^2),\ H = \eta/(1-\eta^2)$
Nakagami$-m$	$\mu = m, \eta \to 0$ or $\eta \to \infty$	$\eta \to \pm 1$
	$\mu = m/2, \eta \to 1$	$\eta \to 0$
Nakagami$-q$ (Hoyt)	$\mu = 0.5, \eta = q^2$	$q^2 = (1-\eta)/(1+\eta)$
Rayleigh	$\mu = 0.5, \eta = 1$	$\mu = 0.5, \eta = 0$

B. Generalized Multipath Fading Channels

It is recalled that the $\eta-\mu$ distribution has been shown to account accurately for small-scale variations of the signal in non-line-of-sight communication scenarios. This fading model is described by the two named parameters, η and μ, and it is valid for two different formats that correspond to two physical models [32]. Given that the instantaneous SNR is given by

$$\gamma = |\alpha|^2 \frac{P}{N_0} \tag{7}$$

the corresponding probability density function (PDF) is defined as [32], [48]

$$f_\gamma(\gamma) = \frac{2\sqrt{\pi}\ \mu^{\mu+\frac{1}{2}}\ h^\mu \gamma^{\mu-\frac{1}{2}}}{\Gamma(\mu) H^{\mu-\frac{1}{2}}\ \overline{\gamma}^{\mu+\frac{1}{2}}} \exp\left(-\frac{2\mu\gamma h}{\overline{\gamma}}\right) I_{\mu-\frac{1}{2}}\left(\frac{2\mu H\gamma}{\overline{\gamma}}\right) \tag{8}$$

where

$$\overline{\gamma} = E(\gamma) = \frac{P\Omega}{N_0} \tag{9}$$

is the average SNR per symbol, with $E(\cdot)$ denoting statistical expectation, and $\Omega = E(|\alpha|^2)$ denotes the corresponding channel variance. Furthermore, $\Gamma(\cdot)$ and $I_n(\cdot)$ denote the Euler gamma function and the modified Bessel function of the first kind, respectively [51]. The parameters h and H are given in terms of η in two formats, as depicted in Table I along with the fading modes that are included in $\eta - \mu$ distribution as special cases. In terms of physical interpretation η denotes the scattered-waves power ratio between the in-phase and quadrature components of the scattered waves in each multipath cluster in Format-1 and the correlation coefficient between the in-phase and quadrature components of each multipath cluster in Format-2. Likewise,

$$\mu = \frac{E^2(\gamma)\,(1 + (H/h)^2)}{2V(\gamma)} \tag{10}$$

is related to multipath clustering in both formats, with $V(\cdot)$ denoting variance operation, respectively [32].

III. EXACT END-TO-END SYMBOL ERROR RATE ANALYSIS

The end-to-end SER for the considered cooperative system can be expressed as [28], [30]

$$P^D_{\text{SER}} = \sum_{z=0}^{2^K-1} P(e|\mathbf{A} = \mathbf{C}_z) P(\mathbf{A} = \mathbf{C}_z) \tag{11}$$

where the binary vector

$$\mathbf{A} = [A(1), A(2), A(3), \ldots, A(K)] \tag{12}$$

of dimension $(1 \times K)$ denotes the state of the relay nodes in the system, with $A(k)$ taking the binary values of 1 and 0 for successful and unsuccessful decoding, respectively. Furthermore,

$$\mathbf{C}_z = [C(1), C(2), C(3), \ldots, C(K)] \tag{13}$$

denotes the different possible decoding combinations of the relays with $z \in \{0, 2^K - 1\}$, where $C(k)$ takes also the value of either 0 or 1. To this effect, for the case of statistically independent channels, the corresponding joint probability of the possible state outcomes can be represented as follows:

$$P(\mathbf{A} = \mathbf{C}_z) = \prod_{k=1}^{K} P(A(k) = C(k)). \tag{14}$$

Notably, the conditional error probability $P(e|\mathbf{A} = \mathbf{C}_z)$ is the error probability conditioned on particular decoding results at relays, while $P(\mathbf{A} = \mathbf{C}_z)$ is the joint probability of the corresponding decoding outcomes. Based on the MRC method, the instantaneous SNR at the destination for given decoding combination, $\mathbf{C}_z$, can be expressed as [30]

$$\gamma_{\text{MRC}}(\mathbf{C}_z) = |\alpha_{S,D}|^2 \frac{P_0}{N_0} + \sum_{k=1}^{K} C(k) |\alpha_{R_k,D}|^2 \frac{P_{R_k}}{N_0}. \tag{15}$$

Furthermore, the MGF for independent fading channels in DF scheme is given by [22], [54]

$$\mathrm{M}_{\gamma_{\text{MRC}}}(s) = M_{\gamma_{S,D}}(s) \prod_{k=1}^{K} M_{\gamma_{R_k,D}}(s) \tag{16}$$

which in the present analysis can be expressed according to [48, eq. (6)], namely

$$M_{\gamma_{\eta-\mu}}\left(\frac{g}{\sin^2\theta}\right) = \left(\frac{4\mu^2 h (2(h+H)\mu + \frac{g}{\sin^2\theta}\bar{\gamma})^{-1}}{(2(h-H)\mu + \frac{g}{\sin^2\theta}\bar{\gamma})}\right)^{\mu}. \tag{17}$$

It is noted that the above expression is particularly useful in the subsequent SER analysis.

A. End-to-End SER for M-PSK Constellations

1) The case of i.n.i.d $\eta - \mu$ Fading Channels: We first evaluate $P(e|\mathbf{A} = \mathbf{C}_z)$ in order to determine (11) for $M-$PSK constellations. To this end, the end-to-end error probability for $M-$PSK constellations over individual $\eta - \mu$ fading link when η, μ and $\bar{\gamma}$ in each path are not necessarily equal can be expressed as [52, eq. (5.78)]

$$\bar{P}_{M-\text{PSK}} = \int_0^{\frac{(M-1)\pi}{M}} \int_0^{\infty} \frac{f_\gamma(\gamma)}{\pi e^{\frac{\gamma g_{\text{PSK}}}{\sin^2\theta}}} \mathrm{d}\gamma \mathrm{d}\theta \tag{18}$$

$$= \underbrace{\frac{1}{\pi}\int_0^{\pi/2} M_\gamma\left(\frac{g_{\text{PSK}}}{\sin^2\theta}\right)\mathrm{d}\theta}_{\triangleq \mathcal{I}_1} + \underbrace{\frac{1}{\pi}\int_{\pi/2}^{\frac{(M-1)\pi}{M}} M_\gamma\left(\frac{g_{\text{PSK}}}{\sin^2\theta}\right)\mathrm{d}\theta}_{\triangleq \mathcal{I}_{11}} \tag{19}$$

where [48]

$$g_{\text{PSK}} = \sin^2\left(\frac{\pi}{M}\right) \tag{20}$$

In order to evaluate (11), we first need to determine the error probability for decoding at the destination terminal, using MRC, under given decoding outcomes at nodes i.e., for a given $\mathbf{C}_z$ [53]. To this end and based on the MGF approach, one obtains (21), shown at the bottom of the page. Evidently, the derivation of an analytic solution for (21) is subject to analytic evaluation of the integrals $\mathcal{I}_1$ and $\mathcal{I}_{11}$. To this end, for the case of non-identical fading parameters, i.e, $\mu_{S,D} \neq \mu_{R_1,D} \neq \cdots \neq \mu_{R_K,D}$, $\eta_{S,D} \neq \eta_{R_1,D} \neq \cdots \neq \eta_{R_K,D}$ and $\overline{\gamma}_{S,D} \neq \overline{\gamma}_{R_1,D} \neq \cdots \neq \overline{\gamma}_{R_k,D}$, the $\mathcal{I}_1$ term can be alternatively expressed as follows

$$\mathcal{I}_1 = \frac{1}{\pi}\int_0^{\pi/2} \frac{1}{\left(1 + \frac{A_1}{\sin^2\theta}\right)^{\mu_{S,D}} \left(1 + \frac{A_2}{\sin^2\theta}\right)^{\mu_{S,D}}} \times \prod_{k=1}^{K} \frac{\mathrm{d}\theta}{\left(1 + \frac{B_{1k}}{\sin^2\theta}\right)^{\mu_{R_k,D}} \left(1 + \frac{B_{2k}}{\sin^2\theta}\right)^{\mu_{R_k,D}}} \tag{22}$$

where

$$\begin{Bmatrix} A_1 \\ A_2 \end{Bmatrix} = \frac{\overline{\gamma}_{S,D} g_{\text{PSK}}}{2(h_{S,D} \{\mp\} H_{S,D})\mu_{S,D}} \tag{23}$$

$$\begin{aligned} P(e|\mathbf{A} = \mathbf{C}_z) = \frac{1}{\pi}\int_0^{\pi/2} & \left(\frac{4\mu_{S,D}^2 h_{S,D}(2(h_{S,D} + H_{S,D})\mu_{S,D} + \frac{g_{\text{PSK}}}{\sin^2\theta}\bar{\gamma}_{S,D})^{-1}}{(2(h_{S,D} - H_{S,D})\mu_{S,D} + \frac{g_{\text{PSK}}}{\sin^2\theta}\bar{\gamma}_{S,D})}\right)^{\mu_{S,D}} \\ & \times \prod_{k=1}^{K}\left(\frac{4\mu_{R_k,D}^2 h_{R_k,D}\,(2(h_{R_k,D} - H_{R_k,D})\mu_{R_k,D} + \frac{g_{\text{PSK}}}{\sin^2\theta}\bar{\gamma}_{R_k,D})^{-1}}{2(h_{R_k,D} + H_{R_k,D})\mu_{R_k,D} + \frac{g_{\text{PSK}}}{\sin^2\theta}\bar{\gamma}_{R_k,D}}\right)^{\mu_{R_k,D}} \mathrm{d}\theta \\ + \frac{1}{\pi}\int_{\pi/2}^{\frac{(M-1)\pi}{M}} & \left(\frac{4\mu_{S,D}^2 h_{S,D}(2(h_{S,D} + H_{S,D})\mu_{S,D} + \frac{g_{\text{PSK}}}{\sin^2\theta}\bar{\gamma}_{S,D})^{-1}}{(2(h_{S,D} - H_{S,D})\mu_{S,D} + \frac{g_{\text{PSK}}}{\sin^2\theta}\bar{\gamma}_{S,D})}\right)^{\mu_{S,D}} \\ & \times \prod_{k=1}^{K}\left(\frac{4\mu_{R_k,D}^2 h_{R_k,D}\,(2(h_{R_k,D} - H_{R_k,D})\mu_{R_k,D} + \frac{g_{\text{PSK}}}{\sin^2\theta}\bar{\gamma}_{R_k,D})^{-1}}{(2(h_{R_k,D} + H_{R_k,D})\mu_{R_k,D} + \frac{g_{\text{PSK}}}{\sin^2\theta}\bar{\gamma}_{R_k,D})}\right)^{\mu_{R_k,D}} \mathrm{d}\theta \end{aligned} \tag{21}$$

and

$$\begin{Bmatrix} B_{1k} \\ B_{2k} \end{Bmatrix} = \frac{\overline{\gamma}_{R_k,D}\, g_{\rm PSK}}{2(h_{R_k,D}\{\mp\}H_{R_k,D})\mu_{R_k,D}}. \tag{24}$$

By also setting $u = \sin^2(\theta)$ and carrying out tedious but basic algebraic manipulations, one obtains

$$\mathcal{I}_1 = \frac{\beta_{\gamma_{\rm MRC}}(g_{\rm PSK})}{2\pi} \int_0^1 \frac{(1-u)^{-\frac{1}{2}} u^{2(\mu_{S,D}+\sum_{k=1}^{K} C(k)\mu_{R_k,D})-\frac{1}{2}}}{\left(1+\frac{u}{A_1}\right)^{\mu_{S,D}} \left(1+\frac{u}{A_2}\right)^{\mu_{S,D}}} \times \prod_{k=1}^{K} \frac{{\rm d}u}{\left(1+\frac{u}{B_{1k}}\right)^{\mu_{R_k,D}} \left(1+\frac{u}{B_{2k}}\right)^{\mu_{R_k,D}}} \tag{25}$$

where

$$\beta_{\gamma_{\rm MRC}}(g_{\rm PSK}) = \left(\frac{4\mu_{S,D}^2(h_{S,D}^2 - H_{S,D}^2)}{\overline{\gamma}_{S,D}^2 g_{\rm PSK}^2}\right)^{\mu_{S,D}} \times \prod_{k=1}^{K} \left(\frac{4\mu_{R_k,D}^2(h_{R_k,D}^2 - H_{R_k,D}^2)}{\overline{\gamma}_{R_k,D}^2 g_{\rm PSK}^2}\right)^{\mu_{R_k,D}}. \tag{26}$$

Importantly, equation (25) can be expressed explicitly in terms of [56, eq. (7.2.4.57)], yielding (27), shown at the bottom of the page, where $F_D^{(n)}(\cdot)$ denotes the generalized Lauricella hypergeometric function of n variables [55].

In the same context, for the $\mathcal{I}_{11}$ integral we set

$$u = \frac{\cos^2(\theta)}{\cos^2(\pi/M)} \tag{28}$$

in (21) yielding

$$\mathcal{I}_{11} = \frac{M_{\gamma_{\rm MRC}}(g_{\rm PSK})\cos(\pi/M)}{2\pi} \times \int_0^1 \frac{u^{-\frac{1}{2}}(1-\cos^2(\pi/M)u)^{2(\mu_{S,D}+\sum_{k=1}^{K} C(k)\mu_{R_k,D})-\frac{1}{2}}}{\left(1-\frac{\cos^2(\pi/M)}{1+A_1}u\right)^{\mu_{S,D}} \left(1-\frac{\cos^2(\pi/M)}{1+A_2}u\right)^{\mu_{S,D}}} \times \prod_{k=1}^{K} \frac{\left(1-\frac{\cos^2(\pi/M)}{1+B_{2k}}u\right)^{-\mu_{R_k,D}}}{\left(1-\frac{\cos^2(\pi/M)}{1+B_{1k}}u\right)^{\mu_{R_k,D}}} {\rm d}u. \tag{29}$$

Evidently, the above integral can be also expressed in terms of the $F_D^{(n)}(\cdot)$ function; therefore, by performing the necessary change of variables and substituting in (29) yields (30), at the bottom of the page.

It is noted here that the $F_D^{(n)}(\cdot)$ function has been studied extensively over the past decades. Nevertheless, despite its undoubted importance it is not unfortunately included as built-in function in popular software packages such as MATLAB, MATHEMATICA and MAPLE. Based on this, a simple MATLAB algorithm for computing this function straightforwardly is proposed in Appendix I.

$$\mathcal{I}_1 = \frac{\beta_{\gamma_{\rm MRC}}(g_{\rm PSK})\Gamma(2\mu_{S,D} + 2\sum_{k=1}^{K} C(k)\mu_{R_k,D} + \frac{1}{2})}{2\sqrt{\pi}\,\Gamma(2\mu_{S,D} + 2\sum_{k=1}^{K} C(k)\mu_{R_k,D} + 1)} \times F_D^{(2K+2)}\Bigg(2\mu_{S,D} + 2\sum_{k=1}^{K} C(k)\mu_{R_k,D} + \frac{1}{2}; \mu_{S,D}, \mu_{S,D}, \mu_{R_1,D}, \ldots, \mu_{R_K,D}, \mu_{R_1,D}, \ldots, \mu_{R_K,D}; 2\mu_{S,D} + 2\sum_{k=1}^{K} C(k)\mu_{R_k,D} + 1; -\frac{1}{A_1}, -\frac{1}{A_2}, -\frac{1}{B_{11}}, \ldots, -\frac{1}{B_{1K}}, -\frac{1}{B_{21}}, \ldots, -\frac{1}{B_{2,K}}\Bigg) \tag{27}$$

$$\mathcal{I}_{11} = \frac{M_{\gamma_{\rm MRC}}(g_{\rm PSK})}{\pi} \times F_D^{(2K+3)}\Bigg(\frac{1}{2}; \mu_{S,D}, \mu_{S,D}, \mu_{R_1,D}, \ldots, \mu_{R_K,D}, \mu_{R_1,D}, \ldots, \mu_{R_K,D}, \frac{1}{2} - 2\mu_{S,D} - 2\sum_{k=1}^{K} C(k)\mu_{R_K,D}; \frac{3}{2}; \frac{\cos^2(\pi/M)}{1+A_1}, \frac{\cos^2(\pi/M)}{1+A_2}, \frac{\cos^2(\pi/M)}{1+B_{11}}, \ldots, \frac{\cos^2(\pi/M)}{1+B_{1K}}, \frac{\cos^2(\pi/M)}{1+B_{21}}, \ldots, \frac{\cos^2(\pi/M)}{1+B_{2K}}, \cos^2(\pi/M)\Bigg) \tag{30}$$

$$\mathcal{I}_{1{\rm i.i.d}} = \frac{\beta_{\gamma_{\rm MRC}}(g_{\rm PSK})\Gamma\left(2\mu_{S,D} + 2\mu_{R,D}\sum_{k=1}^{K} C(k) + \frac{1}{2}\right)}{2\sqrt{\pi}\,\Gamma\left(2\mu_{S,D} + 2\mu_{R,D}\sum_{k=1}^{K} C(k) + 1\right)} F_D^{(4)}\Bigg(2\mu_{S,D} + 2\mu_{R,D}\sum_{k=1}^{K} C(k) + \frac{1}{2}; \mu_{S,D}, \mu_{S,D}, K\mu_{R,D}, K\mu_{R,D}; 2\mu_{S,D} + 2\mu_{R,D}\sum_{k=1}^{K} C(k) + 1; -\frac{1}{A_1}, -\frac{1}{A_2}, -\frac{1}{B_1}, -\frac{1}{B_2}\Bigg) \tag{31}$$

$$\mathcal{I}_{11{\rm i.i.d}} = \frac{M_{\gamma_{\rm MRC}}(g_{\rm PSK})}{\pi} F_D^{(5)}\Bigg(\frac{1}{2}; \mu_{S,D}, \mu_{S,D}, K\mu_{R,D}, K\mu_{R,D}, \frac{1}{2} - 2\mu_{S,D} - 2\mu_{R,D}\sum_{k=1}^{K} C(k); \frac{3}{2}; \frac{\cos^2(\pi/M)}{1+A_1}, \frac{\cos^2(\pi/M)}{1+A_2}, \frac{\cos^2(\pi/M)}{1+B_1}, \frac{\cos^2(\pi/M)}{1+B_2}, \cos^2(\pi/M)\Bigg) \tag{32}$$

2) The Case of i.i.d $\eta-\mu$ Fading Channels: For the special case of identical relay to destination paths i.e., $\mu_{R_1,D} = \cdots = \mu_{R_K,D} = \mu_{R,D}$, $\eta_{R_1,D} = \cdots = \eta_{R_K,D} = \eta_{R,D}$, $\overline{\gamma}_{R_1,D} = \cdots = \overline{\gamma}_{R_K,D} = \overline{\gamma}_{R,D}$ and thus, $B_{11} = \cdots = B_{1K} = B_1$, and $B_{21} = \cdots = B_{2K} = B_2$, equations (27) and (30) can be readily simplified to (31) and (32), respectively, shown at the bottom of the previous page. As a result, with the aid of the derived expressions for $\mathcal{I}_1$ and $\mathcal{I}_{11}$, the corresponding error probability for $M-$PSK constellations can be determined by

$$P(e|\mathbf{A} = \mathbf{C}_z) = \mathcal{I}_1 + \mathcal{I}_{11}. \tag{33}$$

It is recalled that the derivation of the overall SER also requires the determination of the decoding probability of the relay nodes $P(\mathbf{A} = \mathbf{C}_z)$. This is in fact a direct product of the terms

$$P(\bar{\gamma}_{S,R_k}) = P(A(k) = C(k) = 0) \tag{34}$$

i.e. decoding error at the relays and

$$(1 - P(\bar{\gamma}_{S,R_k})) = P(A(k) = C(k) = 1) \tag{35}$$

i.e. successful decoding at the relays, which, as already mentioned, is a pre-requisite for forwarding re-encoded signals to the destination. Importantly, this can be also determined in closed-form with the aid of the commonly used MGF approach, namely

$$\begin{aligned} P(\bar{\gamma}_{S,R_k}) = &\underbrace{\frac{1}{\pi}\int_0^{\pi/2} M_{\gamma_{S,R_k}}\left(\frac{g_{\text{PSK}}}{\sin^2\theta}\right)\mathrm{d}\theta}_{\triangleq \mathcal{I}_2} \\ &+ \underbrace{\frac{1}{\pi}\int_{\pi/2}^{\frac{(M-1)\pi}{M}} M_{\gamma_{S,R_k}}\left(\frac{g_{\text{PSK}}}{\sin^2\theta}\right)\mathrm{d}\theta}_{\triangleq \mathcal{I}_{22}} \end{aligned} \tag{36}$$

which with the aid of (17) can be equivalently re-written according to (37), shown at the bottom of the page. Notably, the integrals in (37) have similar algebraic form to $\mathcal{I}_1$ and $\mathcal{I}_{11}$ since the difference is the absence of $\mu_{R_k,D}$ terms. As a result, the following exact analytic expressions are deduced

$$\begin{aligned} \mathcal{I}_2 = &\frac{\beta_{\gamma_{S,R_k}}(g_{\text{PSK}})\Gamma(2\mu_{S,R_k} + \frac{1}{2})}{2\sqrt{\pi}\Gamma(2\mu_{S,R_k} + 1)} \times F_D^{(2)}\left(2\mu_{S,R_k} + \frac{1}{2};\right. \\ &\left.\mu_{S,R_k}, \mu_{S,R_k}; 2\mu_{S,R_k} + 1; -\frac{1}{C_1}, -\frac{1}{C_2}\right) \end{aligned} \tag{38}$$

and (39), shown at the bottom of the page, where

$$\begin{Bmatrix} C_1 \\ C_2 \end{Bmatrix} = \frac{\overline{\gamma}_{S,R_k} g_{\text{PSK}}}{2(h_{S,R_k}\{\mp\}H_{S,R_k})} \tag{40}$$

and

$$\beta_{S,R_k}(g_{\text{PSK}}) = \left(\frac{4\mu_{S,R_k}^2(h_{S,R_k}^2 - H_{S,R_k}^2)}{\overline{\gamma}_{S,R_k}^2 g_{\text{PSK}}^2}\right)^{\mu_{S,R_k}}. \tag{41}$$

Therefore, the P_{SER}^D for $M-$PSK is deduced by inserting $P(e|\mathbf{A} = \mathbf{C}_z)$ and $P(\mathbf{A} = \mathbf{C}_z)$ in (11).

To the best of the authors' knowledge, the derived exact analytic expressions are novel.

B. End-to-End SER for M–QAM Constellations

Having derived the SER over i.n.i.d and i.i.d $\eta - \mu$ fading channels for the case of $M-$PSK modulations, we can readily derive the respective SER for the case of $M-$QAM constellations.

1) The Case of i.n.i.d $\eta-\mu$ Fading Channels: In the case of independent but not necessarily identically distributed $\eta - \mu$ fading channels and based on [52, eq. (9.21)], it follows that

$$\begin{aligned} \bar{P}_{M-\text{QAM}} = &\underbrace{\frac{4C}{\pi}\int_0^{\pi/2} M_{\gamma_{\text{MRC}}}\left(\frac{g_{\text{QAM}}}{\sin^2\theta}\right)\mathrm{d}\theta}_{\triangleq \mathcal{I}_3} \\ &- \underbrace{\frac{4C^2}{\pi}\int_0^{\pi/4} M_{\gamma_{\text{MRC}}}\left(\frac{g_{\text{QAM}}}{\sin^2\theta}\right)\mathrm{d}\theta}_{\triangleq \mathcal{I}_4} \end{aligned} \tag{42}$$

where

$$g_{\text{QAM}} = \frac{3}{2(M-1)} \tag{43}$$

and

$$C = 1 - \frac{1}{\sqrt{M}}. \tag{44}$$

Evidently, the derivation of an analytic expression for (42) is subject to analytic evaluation of the two involved integrals. To this end, it is noticed that these integrals have similar algebraic representation as the integrals in (18). Therefore, by following the same methodology as in the case of $M-$PSK constellations, using $u = \sin^2\theta$ and carrying out long but basic algebraic manipulations, the $\mathcal{I}_3$ integral can be expressed according to (45), shown at the bottom of the next page, where the parameters A_1, A_2, B_{1k} and B_{2k} are determined by substituting g_{PSK} with g_{QAM} in (23) and (24), respectively. Likewise, the $\mathcal{I}_4$

$$\begin{aligned} P(A(k) = C(k) = 0) = &\frac{1}{\pi}\int_0^{\pi/2}\left(\frac{4\mu_{S,R_k}^2 h_{S,R_k}\left(2(h_{S,R_k} + H_{S,R_k})\mu_{S,R_k} + \frac{g_{\text{PSK}}}{\sin^2\theta}\bar{\gamma}_{S,R_k}\right)^{-1}}{(2(h_{S,R_k} - H_{S,R_k})\mu_{S,R_k} + \frac{g_{\text{PSK}}}{\sin^2\theta}\bar{\gamma}_{S,R_k})}\right)^{\mu_{S,R_k}}\mathrm{d}\theta \\ &+ \frac{1}{\pi}\int_{\pi/2}^{\frac{(M-1)\pi}{M}}\left(\frac{4\mu_{S,R_k}^2 h_{S,R_k}\left(2(h_{S,R_k} + H_{S,R_k})\mu_{S,R_k} + \frac{g_{\text{PSK}}}{\sin^2\theta}\bar{\gamma}_{S,R_k}\right)^{-1}}{(2(h_{S,R_k} - H_{S,R_k})\mu_{S,R_k} + \frac{g_{\text{PSK}}}{\sin^2\theta}\bar{\gamma}_{S,R_k})}\right)^{\mu_{S,R_k}}\mathrm{d}\theta \end{aligned} \tag{37}$$

$$\mathcal{I}_{22} = \frac{M_{\gamma_{S,R_k}}(g_{\text{PSK}})}{\pi}F_D^{(3)}\left(\frac{1}{2}; \mu_{S,R_k}, \mu_{S,R_k}, \frac{1}{2} - 2\mu_{S,R_k}; \frac{3}{2}; \frac{\cos^2(\pi/M)}{1 + C_1}, \frac{\cos^2(\pi/M)}{1 + C_2}, \cos^2(\pi/M)\right) \tag{39}$$

integral has the same integrand but a different upper limit of integration. Thus, by setting $y = 2u$ and following the same methodology, equation (46) is deduced (shown at the bottom of the page) where $\beta_{\gamma_{\text{MRC}}}(g_{\text{QAM}})$ is obtained by substituting g_{PSK} with g_{QAM} in (26).

2) The case of i.i.d $\eta-\mu$ fading channels: In this simplified scenario, the corresponding solutions for $\mathcal{I}_3$ and $\mathcal{I}_4$ for the case of $M-$QAM constellations can be derived by following the same methodology as in the case of $M-$PSK modulations. To this end, after a necessary change of variables and long but basic algebraic manipulations, one obtains (47) and (48), respectively, shown at the bottom of the page. Hence, the error probability is determined by

$$P(e|\mathbf{A} = \mathbf{C}_z) = \frac{4C}{\pi}\mathcal{I}_3 - \frac{4C^2}{\pi}\mathcal{I}_4. \tag{49}$$

In the same context, the corresponding decoding error probability at the relay nodes is expressed as

$$P(\bar{\gamma}_{S,R_k}) = \frac{4C}{\pi} \underbrace{\int_0^{\pi/2} M_{\gamma_{S,R_k}}\left(\frac{g_{\text{QAM}}}{\sin^2\theta}\right)\mathrm{d}\theta}_{\triangleq \mathcal{I}_5} - \frac{4C^2}{\pi} \underbrace{\int_0^{\pi/4} M_{\gamma_{S,R_k}}\left(\frac{g_{\text{QAM}}}{\sin^2\theta}\right)\mathrm{d}\theta}_{\triangleq \mathcal{I}_6}. \tag{50}$$

$$\mathcal{I}_3 = \frac{\beta_{\gamma_{\text{MRC}}}(g_{\text{QAM}})\sqrt{\pi}\,\Gamma\left(2\mu_{S,D} + 2\sum_{k=1}^{K} C(k)\mu_{R_k,D} + \frac{1}{2}\right)}{2\Gamma\left(2\mu_{S,D} + 2\sum_{k=1}^{K} C(k)\mu_{R_k,D} + 1\right)} \times F_D^{(2K+2)}\left(2\mu_{S,D} + 2\sum_{k=1}^{K} C(k)\mu_{R_k,D} + \frac{1}{2}; \mu_{S,D}, \mu_{S,D}, \mu_{R_1,D}, \cdots, \mu_{R_K,D}, \mu_{R_1,D}, \cdots, \mu_{R_K,D}\right.$$
$$\left.; 2\mu_{S,D} + 2\sum_{k=1}^{K} C(k)\mu_{R_k,D} + 1; -\frac{1}{A_1}, -\frac{1}{A_2}, -\frac{1}{B_{11}}, \cdots, -\frac{1}{B_{1K}}, -\frac{1}{B_{21}}, \cdots, -\frac{1}{B_{2,K}}\right) \tag{45}$$

$$\mathcal{I}_4 = \frac{\beta_{\gamma_{\text{MRC}}}(g_{\text{QAM}})\Gamma(2\mu_{S,D} + 2\sum_{k=1}^{K} C(k)\mu_{R_k,D} + \frac{1}{2})}{\Gamma(2\mu_{S,D} + 2\sum_{k=1}^{K} C(k)\mu_{R_k,D} + \frac{3}{2})2^{2(\mu_{S,D} + \sum_{k=1}^{K} C(k)\mu_{R_k,D}) + \frac{3}{2}}} \times F_D^{(2K+3)}\left(2\mu_{S,D} + 2\sum_{k=1}^{K} C(k)\mu_{R_k,D} + \frac{1}{2}; \mu_{S,D}, \mu_{S,D}, \mu_{R_1,D}, \cdots, \mu_{R_K,D}, \mu_{R_1,D}, \cdots, \mu_{R_K,D}, \frac{1}{2}\right.$$
$$\left.; 2\mu_{S,D} + 2\sum_{k=1}^{K} C(k)\mu_{R_k,D} + \frac{3}{2}; -\frac{1}{2A_1}, -\frac{1}{2A_2}, -\frac{1}{2B_{11}}, \cdots, -\frac{1}{2B_{1K}}, -\frac{1}{2B_{21}}, \cdots, -\frac{1}{2B_{2K}}, \frac{1}{2}\right) \tag{46}$$

$$\mathcal{I}_{3\text{i.i.d}} = \frac{\beta_{\gamma_{\text{MRC}}}(g_{\text{QAM}})\sqrt{\pi}\,\Gamma\left(2\mu_{S,D} + 2\mu_{R,D}\sum_{k=1}^{K} C(k) + \frac{1}{2}\right)}{2\Gamma\left(2\mu_{S,D} + 2\mu_{R,D}\sum_{k=1}^{K} C(k) + 1\right)} F_D^{(4)}\left(2\mu_{S,D} + 2\mu_{R,D}\sum_{k=1}^{K} C(k) + \frac{1}{2};\right.$$
$$\left.\mu_{S,D}, \mu_{S,D}, K\mu_{R,D}, K\mu_{R,D}; 2\mu_{S,D} + 2\mu_{R,D}\sum_{k=1}^{K} C(k) + 1; -\frac{1}{A_1}, -\frac{1}{A_2}, -\frac{1}{B_1}, -\frac{1}{B_2}\right) \tag{47}$$

$$\mathcal{I}_{4\text{i.i.d}} = \frac{\beta_{\gamma_{\text{MRC}}}(g_{\text{QAM}})\Gamma(2\mu_{S,D} + 2\mu_{R,D}\sum_{k=1}^{K} C(k) + \frac{1}{2})}{\Gamma(2\mu_{S,D} + 2\mu_{R,D}\sum_{k=1}^{K} C(k) + \frac{3}{2})2^{2\mu_{S,D} + 2\mu_{R,D}\sum_{k=1}^{K} C(k) + \frac{3}{2}}} F_D^{(5)}\left(2\mu_{S,D} + 2\mu_{R,D}\sum_{k=1}^{K} C(k) + \frac{1}{2};\right.$$
$$\left.\mu_{S,D}, \mu_{S,D}, K\mu_{R,D}, K\mu_{R,D}, \frac{1}{2}; 2\mu_{S,D} + 2\mu_{R_k,D}\sum_{k=1}^{K} C(k) + \frac{3}{2}; -\frac{1}{2A_1}, -\frac{1}{2A_2}, -\frac{1}{2B_1}, -\frac{1}{2B_2}, \frac{1}{2}\right) \tag{48}$$

$$\mathcal{I}_5 = \frac{\beta_{\gamma_{S,R_k}}(g_{\text{QAM}})\sqrt{\pi}\,\Gamma(2\mu_{S,R_k} + \frac{1}{2})}{2\Gamma(2\mu_{S,R_k} + 1)} \times F_D^{(2)}\left(2\mu_{S,R_k} + \frac{1}{2}; \mu_{S,R_k}, +1; -\frac{1}{C_1}, -\frac{1}{C_2}\right) \tag{51}$$

$$\mathcal{I}_6 = \frac{\beta_{\gamma_{S,R_k}}(g_{\text{QAM}})\Gamma(2\mu_{S,R_k} + \frac{1}{2})}{\Gamma(2\mu_{S,R_k} + \frac{3}{2})2^{2\mu_{S,R_k} + \frac{3}{2}}} \times F_D^{(3)}\left(2\mu_{S,R_k} + \frac{1}{2}; \mu_{S,R_k}, \mu_{S,R_k}, \frac{1}{2}; 2\mu_{S,R_k} + \frac{3}{2}; -\frac{1}{2C_1}, -\frac{1}{2C_2}, \frac{1}{2}\right) \tag{52}$$

Based on the approach in (37) and after long but basic algebraic manipulations yields the following analytic expressions for $\mathcal{I}_5$ and $\mathcal{I}_6$, in (51) and (52) (shown at the bottom of the previous page) respectively, where $\beta_{\gamma_{S,R_k}}(g_{\rm QAM})$ is evaluated by substituting $g_{\rm PSK}$ with $g_{\rm QAM}$ in (41), whereas C_1 and C_2 are obtained by substituting $g_{\rm PSK}$ with $g_{\rm QAM}$ in (40). Therefore, using (51) and (52), the corresponding decoding error probability can be readily expressed as

$$P(\bar{\gamma}_{S,R_k}) = P(A(k) = C(k) = 0) \tag{53}$$

$$= \frac{4C}{\pi}\mathcal{I}_5 - \frac{4C^2}{\pi}\mathcal{I}_6. \tag{54}$$

To this effect, an exact analytic expression for the SER is deduced by substituting $P(\mathbf{A} = \mathbf{C}_z)$ in (11) along with the corresponding $P(e|\mathbf{A} = \mathbf{C}_z)$. Notably, this expression can be computed with the aid of the proposed MATLAB algorithm in Appendix I.

C. Simple Asymptotic Expressions

The derivation of asymptotic expressions typically leads to useful insights on the impact of the involved parameters on the system performance. This is also the case in the present analysis as simple analytic expressions are derived for high SNR values. To this end, the MGF of $\eta - \mu$ distribution can be accurately approximated as

$$M_{\gamma_{\eta-\mu}}\left(\frac{g}{\sin^2\theta}\right) = \left(\frac{4\mu^2 h(2(h+H)\mu + \frac{g}{\sin^2\theta}\bar{\gamma})^{-1}}{(2(h-H)\mu + \frac{g}{\sin^2\theta}\bar{\gamma})}\right)^{\mu}$$
$$\approx \left(\frac{4\mu^2 h}{g^2\bar{\gamma}^2}\right)^{\mu}\sin^{4\mu}(\theta). \tag{55}$$

Based on this, the conditional error probability $P(e|\mathbf{A} = \mathbf{C}_z)$ can be approximated as follows:

$$P(e|\mathbf{A} = \mathbf{C}_z) \approx \left(\frac{4\mu_{S,D}^2 h_{S,D}}{g^2\bar{\gamma}_{S,D}^2}\right)^{\mu_{S,D}} \times \prod_{k=1}^{K} A_{R_k,D}(\mathbf{C}_z)\left(\frac{4\mu_{R_k,D}^2 h_{R_k,D}}{g^2\bar{\gamma}_{R_k,D}^2}\right)^{\mu_{R_k,D}} \tag{56}$$

where $A_{R_K,D}(\mathbf{C}_z)$ for $M-$PSK constellations is given by

$$A_{R_K,D}(\mathbf{C}_z) = \frac{1}{\pi}\int_0^{\frac{(M-1)\pi}{\pi}} [\sin(\theta)]^{4(\mu_{S,D}+\sum_{k=1}^{K} C(k)\mu_{R_k,D})}\mathrm{d}\theta \tag{57}$$

which can be equivalently re-written as follows:

$$A_{R_K,D}(\mathbf{C}_z) = \frac{1}{\pi}\underbrace{\int_0^{\pi/2} [\sin(\theta)]^{4(\mu_{S,D}+\sum_{k=1}^{K} C(k)\mu_{R_k,D})}\mathrm{d}\theta}_{\mathcal{I}_7} + \frac{1}{\pi}\underbrace{\int_{\pi/2}^{\frac{(M-1)\pi}{M}} [\sin(\theta)]^{4(\mu_{S,D}+\sum_{k=1}^{K} C(k)\mu_{R_k,D})}\mathrm{d}\theta}_{\mathcal{I}_8}. \tag{58}$$

The derivation of an analytic expression for (56) is subject to evaluation of the above trigonometric integrals. Hence, by setting $u = \sin^2(\theta)$ and

$$a = 2(\mu_{S,D} + \sum_{k=1}^{K} C(k)\mu_{R_k,D}) \tag{59}$$

it follows that

$$\mathcal{I}_7 = \frac{1}{2}\int_0^1 \frac{u^{a-\frac{1}{2}}}{(1-u)^{\frac{1}{2}}}\mathrm{d}u \tag{60}$$

which can be expressed in terms of [51, eq. (3.191.1)]. To this end, by performing the necessary variable transformation and after basic algebraic manipulations one obtains

$$\mathcal{I}_7 = \frac{\sqrt{\pi}\Gamma(2\mu_{S,D} + 2\sum_{k=1}^{K} C(k)\mu_{R_k,D} + \frac{1}{2})}{2\Gamma(2\mu_{S,D} + 2\sum_{k=1}^{K} C(k)\mu_{R_k,D} + 1)}. \tag{61}$$

Likewise, by setting $u = \cos^2(\theta)/\cos^2(\pi/M)$ to the second integral in (57), it follows that

$$\mathcal{I}_8 = \frac{\cos(\pi/M)}{2}\int_0^1 \frac{u^{-\frac{1}{2}}}{\left(1 - u\cos^2\left(\frac{\pi}{M}\right)\right)^{\frac{1}{2}-a}}\mathrm{d}u \tag{62}$$

which can be expressed in terms of the Gauss hypergeometric function ${}_2F_1(\cdot,\cdot;\cdot;\cdot)$ [56], yielding (63), shown at the bottom of the page. To this effect, $A_{R_K,D}(\mathbf{C}_z)$ can be readily expressed as

$$A_{R_K,D}(\mathbf{C}_z) = \frac{\mathcal{I}_7}{\pi} + \frac{\mathcal{I}_8}{\pi}. \tag{64}$$

In the same context, for the case of $M-$QAM constellations one obtains

$$A_{R_K,D}(\mathbf{C}_z) = \frac{4C}{\pi}\underbrace{\int_0^{\pi/2} [\sin(\theta)]^{4(\mu_{S,D}+\sum_{k=1}^{K} C(k)\mu_{R_k,D})}\mathrm{d}\theta}_{\mathcal{I}_9} - \frac{4C^2}{\pi}\underbrace{\int_0^{\pi/4} [\sin(\theta)]^{4(\mu_{S,D}+\sum_{k=1}^{K} C(k)\mu_{R_k,D})}\mathrm{d}\theta}_{\mathcal{I}_{10}}. \tag{65}$$

$$\mathcal{I}_8 = \cos\left(\frac{\pi}{M}\right)\ {}_2F_1\left(\frac{1}{2} - 2\mu_{S,D} + 2\sum_{k=1}^{K} C(k)\mu_{R_k,D}, \frac{1}{2}; \frac{3}{2}; \cos^2\left(\frac{\pi}{M}\right)\right) \tag{63}$$

It is evident that the integrals $\mathcal{I}_7$ and $\mathcal{I}_9$ have the same algebraic forms. Hence, it follows that

$$\mathcal{I}_9 = \frac{\sqrt{\pi}\Gamma(2(\mu_{S,D} + \sum_{k=1}^{K} C(k)\mu_{R_k,D}) + \frac{1}{2})}{2\Gamma(2(\mu_{S,D} + \sum_{k=1}^{K} C(k)\mu_{R_k,D}) + 1)} \tag{66}$$

for the first integral, while and upon setting $u = 2\sin^2(\theta)$ in the second integral, one obtains (67), shown at the bottom of the page. Therefore, with the aid of (66) and (67), the $A_{R_K,D}(\mathbf{C}_z)$ for the case of $M-$QAM constellations is given by

$$A_{R_K,D}(\mathbf{C}_z) = \frac{4C}{\pi}\mathcal{I}_9 - \frac{4C^2}{\pi}\mathcal{I}_{10}. \tag{68}$$

The decoding error probability of the relays also in the high SNR regime can be expressed as

$$P(A(k) = C(k) = 0) \approx A_{S,R_k}\left(\frac{4\mu_{S,R_k}^2 h_{S,R_k}}{g^2\overline{\gamma}_{S,R_k}^2}\right)^{\mu_{S,R_k}} \tag{69}$$

and

$$P(A(k) = C(k) = 1) \approx 1 - A_{S,R_k}\left(\frac{4\mu_{S,R_k}^2 h_{S,R_k}}{g^2\overline{\gamma}_{S,R_k}^2}\right)^{\mu_{S,R_k}} \tag{70}$$

where A_{S,R_k} for $M-$PSK and $M-$QAM constellations is given by

$$A_{S,R_k} = \frac{1}{\pi}\int_0^{\frac{(M-1)\pi}{M}} \sin^{4\mu_{S,R_k}}(\theta)\mathrm{d}\theta \tag{71}$$

and

$$A_{S,R_k} = \frac{4C}{\pi}\int_0^{\pi/2} \sin^{4\mu_{S,R_k}}(\theta)\mathrm{d}\theta - \frac{4C^2}{\pi}\int_0^{\pi/4} \sin^{4\mu_{S,R_k}}(\theta)\mathrm{d}\theta \tag{72}$$

respectively. It is evident that exact analytic expressions for A_{S,R_k}, for both modulation schemes, can be obtained by following the same methodology and procedure as in the previous case yielding

$$A_{S,R_k} = \frac{\Gamma(2\mu_{S,R_k} + \frac{1}{2})}{2\sqrt{\pi}\Gamma(2\mu_{S,R_k} + 1)} + \frac{\cos(\pi/M)}{\pi}\, {}_2F_1\left(\frac{1}{2} - 2\mu_{S,R_k}, \frac{1}{2}; \frac{3}{2}; \cos^2(\pi/M)\right) \tag{73}$$

for the case of $M-$PSK and

$$A_{S,R_k} = \frac{2C\Gamma(2\mu_{S,R_k} + \frac{1}{2})}{\sqrt{\pi}\Gamma(2\mu_{S,R_k} + 1)} - \frac{C^2\Gamma(2\mu_{S,R_k} + \frac{1}{2})\, {}_2F_1\left(\frac{1}{2}, 2\mu_{S,R_k} + \frac{1}{2}; 2\mu_{S,R_k} + \frac{3}{2}; \frac{1}{2}\right)}{\pi 2^{2\mu_{S,R_k}+\frac{1}{2}}\ \Gamma(2\mu_{S,R_k} + \frac{3}{2})} \tag{74}$$

for the case of $M-$QAM. It is noted here that at sufficiently high SNR, the probability $P(A(k) = C(k) = 0)$ is clearly smaller than unity and thus,

$$1 - A_{S,R_k}\left(\frac{4\mu_{S,R_k}^2 h_{S,R_k}}{(g^2\overline{\gamma}_{S,R_k}^2}\right)^{\mu_{S,R_k}} \simeq 1. \tag{75}$$

To this effect and by substituting (56) and (69) into (11), the SER of the multi-relay regenerative system over generalized fading channels at the high SNR regime can be expressed as

$$P_{\mathrm{SER}}^{D} \approx \left(\frac{4\mu_{S,D}^2 h_{S,D}}{g^2\overline{\gamma}_{S,D}^2}\right)^{\mu_{S,D}} \times \sum_{z=0}^{2^K-1}\prod_{k=1}^{K} A_{R_k,D}(\mathbf{C}_z)\left(\frac{4\mu_{R_k,D}^2 h_{R_k,D}}{g^2\overline{\gamma}_{R_k,D}^2}\right)^{\mu_{R_k,D}} \times \prod_{k=1}^{K} A_{S,R_k}\left(\frac{4\mu_{S,R_k}^2 h_{S,R_k}}{g^2\overline{\gamma}_{S,R_k}^2}\right)^{\mu_{S,R_k}} \tag{76}$$

where g corresponds to either $g_{\mathrm{PSK}} = \sin^2(\pi/M)$ or $g_{\mathrm{QAM}} = 3/(2(M-1))$ according to (18) and (42), respectively, depending on the selected modulation scheme.

D. Amount of Fading

It is recalled that the amount of fading (AoF) is a useful metric for quantifying the fading severity in different communication scenarios and is defined according to [52, eq. (1.27)], namely

$$\mathrm{AoF} = \frac{\mathrm{Var}(\gamma_{\mathrm{MRC}})}{(\mathrm{E}(\gamma_{\mathrm{MRC}}))^2} \tag{77}$$

$$= \frac{\mathrm{E}(\gamma_{\mathrm{MRC}}^2) - (\mathrm{E}(\gamma_{\mathrm{MRC}}))^2}{(\mathrm{E}(\gamma_{\mathrm{MRC}}))^2}. \tag{78}$$

The n^{th} moment of the γ_{MRC} in the considered setup can be determined by [54], yielding

$$\mu_n = (-1)^n\left[\frac{d^n}{ds^n}\left(M_{\gamma_{S,D}}(s)\prod_{k=1}^{K} M_{R_k,D}(s)\right)\right]_{s=0}. \tag{79}$$

Based on this, the first two moments in (79) are obtained for $n = 1$ and $n = 2$, namely,

$$\mathrm{E}(\gamma_{\mathrm{MRC}}) = \frac{\partial \mathrm{M}_{\gamma_{\mathrm{MRC}}}(s)}{\partial s}|_{s=0} \tag{80}$$

and

$$\mathrm{E}(\gamma_{\mathrm{MRC}}^2) = \frac{\partial^2 \mathrm{M}_{\gamma_{\mathrm{MRC}}}(s)}{\partial^2 s}|_{s=0}. \tag{81}$$

$$\mathcal{I}_{10} = \frac{2^{-(2\mu_{S,D}+\frac{3}{2})}\, {}_2F_1\left(\frac{1}{2}, 2\mu_{S,D} + 2\sum_{k=1}^{K} C(k)\mu_{R_k,D} + \frac{1}{2}; 2\mu_{S,D} + 2\sum_{k=1}^{K} C(k)\mu_{R_k,D} + \frac{3}{2}; \frac{1}{2}\right)}{2^{2\sum_{k=1}^{K} C(k)\mu_{R_k,D}}\ \Gamma(2\mu_{S,D} + 2\sum_{k=1}^{K} C(k)\mu_{R_k,D} + \frac{3}{2})[\Gamma(2\mu_{S,D} + 2\sum_{k=1}^{K} C(k)\mu_{R_k,D} + \frac{1}{2})]^{-1}} \tag{67}$$

To this effect and recalling (15)–(17), as well as carrying out long but basic algebraic manipulations, the corresponding AoF for i.i.d channels, if all relays decode correctly, can be expressed as follows:

$$\mathrm{AoF} = \frac{\mu_{S,D}(\mu_{S,D}+1)\delta_1^2 - 2\delta_2\mu_{S,D} - 2\delta_3 K\mu_{R,D}}{(\mu_{S,D}\delta_1 + K\mu_{R,D}\delta_4)^2} + \frac{\mu_{R,D}(K\mu_{R,D}+1)\delta_4^2 + 2\mu_{S,D}\mu_{R,D}\delta_1\delta_4}{(\mu_{S,D}\delta_1 + K\mu_{R,D}\delta_4)^2 K^{-1}} - 1 \quad (82)$$

where

$$\delta_1 = \frac{\overline{\gamma}_{S,D} h_{S,D}}{\mu_{S,D}(h_{S,D}^2 - H_{S,D}^2)}, \quad (83)$$

$$\delta_2 = \frac{\overline{\gamma}_{S,D}^2}{4\mu_{S,D}^2(h_{S,D}^2 - H_{S,D}^2)}, \quad (84)$$

$$\delta_3 = \frac{\overline{\gamma}_{R,D}^2}{4\mu_{R,D}^2(h_{R,D}^2 - H_{R,D}^2)} \quad (85)$$

and

$$\delta_4 = \frac{\overline{\gamma}_{R,D} h_{R,D}}{\mu_{R,D}(h_{R,D}^2 - H_{R,D}^2)}. \quad (86)$$

By recalling that the $\eta - \mu$ fading model includes as special cases the Nakagami$-m$, Hoyt and Rayleigh distributions, the corresponding AoF for these cases can be readily deduced accordingly.

IV. Power Allocation Analysis

Equal power allocation (EPA) is not an optimal scheme for distributing the available total transmission power between the source and relay nodes, particularly when the involved channels are highly unbalanced. Hence, the main aim of this section is to analyze and compare the performance of the considered cooperative system under generalized fading channels, with EPA and OPA, under the assumption of total sum-power constraint. Opposed to single-device implementation perspective and the corresponding per node power constraint, the considered approach is more of a network or system view from the optimization perspective, seeking to understand and quantify the potential gain in the end-to-end BER/SER performance if the total power is allocated more efficiently compared to the baseline EPA scheme. To this effect, we derive the OPA strategy that minimizes the derived asymptotic SER of the considered regenerative system subject to the sum-power constraint of a power budget P. It is noted here that only partial knowledge of the channel state information (CSI) is required for employing the OPA scheme [26], [28]. The derived SER expression in (76) is a function of the powers allocated at the source and the K relays of the system while the available power should be allocated optimally in order to enhance the end-to-end quality of the transmission[3].

[3]Without loss of generality, the considered OPA can be practically controlled by a centralized management or power allocation unit.

Based on the above, the corresponding non-linear optimization problem can be formulated as follows:

$$\mathbf{a_{opt}} = \arg\min_{\mathbf{a}} P_{\mathrm{SER}}^{D}$$

$$\text{Subject to}: \quad a_0 + \sum_{k=1}^{K} a_{R_k} = 1, \quad a_0 \geq 0, a_{R_k} \geq 0 \quad (87)$$

where

$$\mathbf{a} = [a_0, a_{R_1}, a_{R_2}, \ldots, a_{R_k}] \quad (88)$$

denotes the relative power allocation vector. Importantly, the cost function in (87) is convex in the parameters a_0 and a_{R_k} over the feasible set defined by linear power ratio constraints. The corresponding proof is provided in Appendix II. To this effect and following the definitions in [57], the Lagrangian of this optimization problem is given by

$$L = P_{\mathrm{SER}}^{D} + \lambda\left(a_0 + \sum_{k=1}^{K} a_{R_k} - 1\right) - \mu_0 a_0 - \sum_{k=1}^{K} \mu_k a_{R_k} \quad (89)$$

where λ denotes the Lagrange multiplier satisfying the power constraint, whereas μ_0 and μ_k parameters serve as slack variables. The nonlinear optimization problem in (87) can be solved using e.g. a line search method. However, to develop some insights for the power allocation policy we apply the Karush-Kuhn-Tucker (KKT) conditions for minimizing the corresponding SER [57]. To this end, it immediately follows that all μ_k and μ_0 parameters are zero while the following first derivatives form the necessary condition for maximizing the performance of the system

$$\frac{\partial P_{\mathrm{SER}}^{D}}{\partial a_0} = \frac{\partial P_{\mathrm{SER}}^{D}}{\partial a_{R_k}}, \qquad (1 \leq k \leq K) \quad (90)$$

In order to obtain feasible relations between asymptotically optimal powers of the cooperating nodes, we employ the asymptotic SER in (76). Hence, by re-writing this in terms of the power ratios allocated at the transmitting nodes it follows that

$$P_{\mathrm{SER}}^{D} \approx \left(\frac{4\mu_{S,D}^2 h_{S,D} N_0^2}{g^2 a_0^2 \Omega_{S,D}^2 P^2}\right)^{\mu_{S,D}} \times \sum_{z=0}^{2^K-1} \prod_{k=1}^{K} A_{R_K,D}(\mathbf{C}_z)\left(\frac{4\mu_{R_k,D}^2 h_{R_k,D} N_0^2}{a_{R_k}^2 g^2 \Omega_{R_k,D}^2 P^2}\right)^{\mu_{R_k,D}} \times \prod_{k=1}^{K} A_{S,R_k}\left(\frac{4\mu_{S,R_k}^2 h_{S,R_k} N_0^2}{a_0^2 g^2 \Omega_{S,R_k}^2 P^2}\right)^{\mu_{S,R_k}}. \quad (91)$$

In order to derive an optimal power allocation policy for the DF protocol, we initially restrict our scenario to $K = 1$ and $K = 2$ relay nodes and then we generalize the result for K relays.

1) K = 1 Scenario: The possible decoding sets in this case are $C_0 = 0$ i.e., the relay is unable to decode correctly, and $C_1 = 1$ i.e. the relay decodes successfully. Thus, using (91) and neglecting the constant term outside the summation after factoring out a_0, it follows that

$$\min\left[\frac{K_1}{a_0^{2(\mu_{S,D}+\mu_{S,R_1})}}+\frac{K_2}{a_0^{2\mu_{S,D}}a_{R_1}^{2\mu_{R_1,D}}}\right]$$
$$\text{Subject to}: a_0+a_{R_1}=1 \tag{92}$$

where

$$K_1 = A_{S,D}A_{S,R_1}\left(\frac{4\mu_{S,R_1}^2 h_{S,R_1}N_0^2}{g^2\Omega_{S,R_1}^2 P^2}\right)^{\mu_{S,R_1}} \tag{93}$$

and

$$K_2 = A_{R1,D}(C_1)\left(\frac{4\mu_{R_1,D}^2 h_{R_1,D}N_0^2}{g^2\Omega_{R_1,D}^2 P^2}\right)^{\mu_{R_1,D}}. \tag{94}$$

Next, we apply the necessary condition in (90) to determine the relation between optimal power allocations in the two nodes. Thus, the first derivative of P_{SER}^D with respect to a_0 is expressed as

$$\frac{\partial P_{\text{SER}}^D}{\partial a_0} = -\frac{2(\mu_{S,D}+\mu_{S,R_1})K_1}{a_0^{2(\mu_{S,D}+\mu_{S,R_1})+1}} - \frac{2\mu_{S,D}K_2}{a_0^{2\mu_{S,D}+1}a_{R_1}^{2\mu_{R_1,D}}} \tag{95}$$

whereas the first derivative with respect to a_{R_1} is given by

$$\frac{\partial P_{\text{SER}}^D}{\partial a_{R_1}} = -\frac{2\mu_{R_1,D}K_2}{a_0^{2\mu_{S,D}}a_{R_1}^{2\mu_{R_1,D}+1}}. \tag{96}$$

Equating the above two relations and after some long but basic rearrangements, it follows that

$$\frac{(\mu_{S,D}+\mu_{S,R_1})K_1}{K_2} = \frac{a_0^{2\mu_{S,R_1}+1}}{a_{R_1}^{2\mu_{R_1,D}}}\left(\frac{\mu_{R_1,D}}{a_{R_1}}-\frac{\mu_{S,D}}{a_0}\right). \tag{97}$$

It is noticed that the left-hand side of (97) depends only on the channel parameters. As a result, this term is always positive which implies directly a power policy of

$$a_0\mu_{R_1,D} \;\geq\; a_{R_1,D}\mu_{S,D}. \tag{98}$$

These relations are also in agreement with the power allocation over Rayleigh, Nakagami$-m$, and Hoyt (Nakagami$-q$) fading distributions under the special cases given in Section III. Closed-form expressions for the power ratios for arbitrary values of μ_{S,R_1} and $\mu_{R_1,D}$ are mathematically intractable. However, for $\mu_{S,R_1}=\mu_{R_1,D}=\mu$ and assigning $\zeta = a_0/a_{R_1}$, equation (97) can be written as

$$\mu\zeta^{2\mu+1} - \mu_{S,D}\zeta^{2\mu} - \frac{(\mu_{S,D}+\mu)K_1}{K_2} = 0. \tag{99}$$

The above polynomial equation can be solved for $2\mu \in \mathbb{Z}$. Specifically, for $2\mu = 1$ and using the power constraint closed-form expressions for the optimal powers transmitted at the source and relay nodes can be expressed as

$$P_0 = \frac{\mu_{S,D}+\sqrt{\mu_{S,D}^2+(1+2\mu_{S,D})K_1/K_2}}{1+\mu_{S,D}+\sqrt{\mu_{S,D}^2+(1+2\mu_{S,D})K_1/K_2}}P \tag{100}$$

and

$$P_{R_1} = \frac{1}{1+\mu_{S,D}+\sqrt{\mu_{S,D}^2+(1+2\mu_{S,D})K_1/K_2}}P \tag{101}$$

respectively. Closed-form expressions for the optimal powers for higher values of 2μ can be obtained by evaluating (99) using mathematical softwares, such as MATLAB, MATHEMATICA and MAPLE.

2) $K = 2$ Scenario: In this case, the following four scenarios are valid: $\mathbf{C}_0 = (0, 0)$ when the two relays decode incorrectly; $\mathbf{C}_1 = (0, 1)$ when the first relay decodes incorrectly and the second relay decodes successfully; $\mathbf{C}_2 = (1, 0)$ when the first relay decodes successfully and the second relay decodes incorrectly; and $\mathbf{C}_3 = (1, 1)$ when both relays decode successfully. Based on this, the corresponding optimization problem can be expressed as follows

$$\min\left[\frac{K_3}{a_0^{2(\mu_{S,D}+\mu_{S,R_1}+\mu_{S,R_2})}}+\frac{K_4}{a_0^{2(\mu_{S,D}+\mu_{S,R_1})}a_{R_2}^{2\mu_{R_2,D}}}\right.$$
$$\left.+\frac{K_5}{a_0^{2(\mu_{S,D}+\mu_{S,R_2})}a_{R_1}^{2\mu_{R_1,D}}}+\frac{K_6}{a_0^{2\mu_{S,D}}a_{R_2}^{2\mu_{R_2,D}}a_{R_1}^{2\mu_{R_1,D}}}\right]$$
$$\text{Subject to}: a_0+a_{R_1}+a_{R_2}=1 \tag{102}$$

where K_3, K_4, K_5 and K_6 relate to the channel parameters, which are not affecting the sign of the derivatives in any case. To this effect, the derivative of P_{SER}^D with respect to a_{R_1} is given by

$$\frac{\partial P_{\text{SER}}^D}{\partial a_{R_1}} = -\frac{2K_5\mu_{R_1,D}}{a_0^{2(\mu_{S,D}+\mu_{S,R_2})}a_{R_1}^{2\mu_{R_1,D}+1}} - \frac{2K_6\mu_{R_1,D}}{a_0^{2\mu_{S,D}}a_{R_2}^{2\mu_{R_2,D}}a_{R_1}^{2\mu_{R_1,D}+1}}, \tag{103}$$

whereas the derivative of P_{SER}^D with respect to a_{R_2} is given by

$$\frac{\partial P_{\text{SER}}^D}{\partial a_{R_2}} = -\frac{2K_4\mu_{R_2,D}}{a_0^{2(\mu_{S,D}+\mu_{S,R_1})}a_{R_2}^{2\mu_{R_2,D}+1}} - \frac{2K_6\mu_{R_2,D}}{a_0^{2\mu_{S,D}}a_{R_2}^{2\mu_{R_2,D}+1}a_{R_1}^{2\mu_{R_1,D}}}. \tag{104}$$

With the aid of the above two representations and assuming same channel conditions, i.e. $\mu_{S,R_1}=\mu_{S,R_2}$, $\eta_{S,R_1}=\eta_{S,R_2}$, $\Omega_{S,R_1}=\Omega_{S,R_2}$, $\mu_{R_1,D}=\mu_{R_2,D}$, $\eta_{R_1,D}=\eta_{R_2,D}$, and $\Omega_{R_1,D}=\Omega_{R_2,D}$, a power allocation strategy can be proposed as $a_{R_1}=a_{R_2}$. Likewise, by recalling that

$$\frac{\partial P_{\text{SER}}^D}{\partial a_{R_k}} = \frac{\partial P_{\text{SER}}^D}{\partial a_{R_{k+1}}} \tag{105}$$

it is straightforwardly shown that

$$a_{R_k} = a_{R_{k+1}}. \tag{106}$$

The power assignment indicates that under the total power constraint and the assumed channel conditions for the regenerative

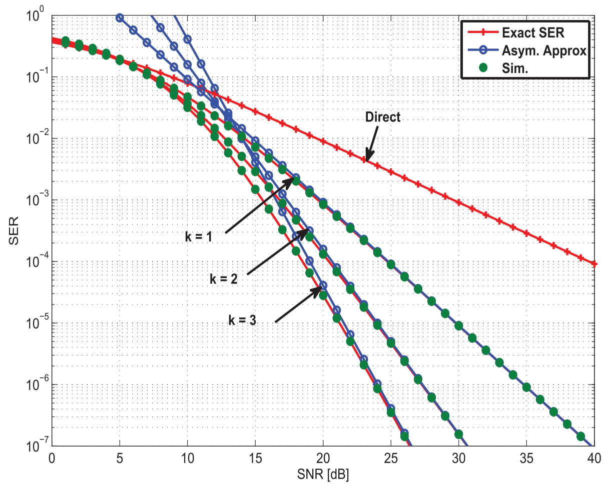

Fig. 2. SER in $\eta-\mu$ fading with $\mu=0.5, \eta=1$ and $\Omega_{S,D}=\Omega_{S,R_k}=\Omega_{R_k,D}=0\,\text{dB}$ for 4−PSK/4−QAM constellation with different number of relays and EPA.

TABLE II
DIVERSITY GAINS FOR ONE, TWO AND THREE RELAYS USING 4-PSK/4-QAM FOR $\mu=0.5$ AND $\eta=1$

K	Diversity Gain (Exact)	Diversity Gain (Asymp.)
1	1.96	2
2	2.91	3
3	3.85	4

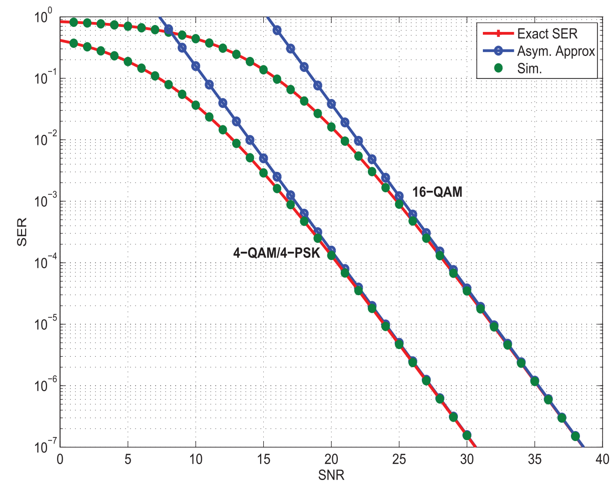

Fig. 3. SER in $\eta-\mu$ fading with $\mu=0.5, \eta=1$ and $\Omega_{S,D}=\Omega_{S,R_k}=\Omega_{R_k,D}=0\,\text{dB}$ for 4−QAM/4−PSK and 16−QAM, $K=2$ and EPA.

network, power control mechanism with the relays is not essential, but the remaining power left from the total power budget after the source can be simply allocated uniformly between the nodes. This is further elaborated and largely verified in the following section.

V. NUMERICAL RESULTS

In this Section, the offered analytic results are employed in evaluating the performance of the considered regenerative system for different communication scenarios. To this end, the variance of the noise is assumed to be normalized as $N_0=1$ for all considered scenarios while transmit powers are equally or optimally allocated to the source and the relays. It is also noted that the presented results are limited to Format−1 of the $\eta-\mu$ distribution but they can be readily extended to scenarios that correspond to Format−2 [32].

Fig. 2 illustrates the SER performance as a function of SNR for one, two and three relays using EPA, i.e.,

$$P_0 = P_{R_k} = \frac{P}{K+1} \tag{107}$$

over symmetric and balanced $\eta-\mu$ fading channels for 4−PSK/4−QAM constellation. Also, the $\eta-\mu$ fading parameters are $\mu=0.5$ and $\eta=1$ while Ω parameters are equal to unity. It is evident that the results from the exact analytic expressions are in excellent agreement with the respective results from computer simulations, which verifies their validity. It is also shown that the exact results are bounded tightly by the corresponding asymptotic curves in the range from moderate SNR values to the to high SNR regime while a full diversity order i.e., 2, 3 and 4, can be respectively achieved. Table II depicts the corresponding diversity gains computed from the slopes for the exact and asymptotic curves along with the direct transmission scenario, for reference, where it is assumed that $P_0=P$. It is observed that at a target SER of 10^{-4} the single relay system exhibits a gain of 15dB over the direct transmission, whereas the two and three relay systems outperform the direct scenario by about 19.5dB and 21.5dB, respectively. In the same context, Fig. 3 shows the SER performance as a function of SNR for 4−QAM/4−PSK and 16−QAM constellations for the case of two relays with EPA over symmetric $\eta-\mu$ fading channels with $\mu=0.5$ and $\eta=1$ as well as balanced links i.e., $\Omega_{S,D}=\Omega_{S,R_k}=\Omega_{R_k,D}=\Omega=0$dB. It is also shown that the exact results are again in tight agreement with the respective simulation results and that the asymptotic curves are tending to be practically identical to the exact ones for SERs lower than 10^{-3}. Therefore, it becomes evident that in practical system designs of DF relaying at the high SNR regime, the offered asymptotic expressions can provide useful insights on the system performance.

Fig. 4 illustrates the cooperation performance of 4−QAM/QPSK system in a two relay scenario for $\mu=\{0.5, 1, 1.5\}$ and identical channel variance of $\Omega_{S,D}=\Omega_{S,R_k}=\Omega_{R_k,D}=0$dB with EPA. It is also recalled that the case of $\mu=0.5$ corresponds to the Nakagami−q (Hoyt) distribution with $q^2=\eta$. By varying the value of η, we observe the effect of the scattered-wave power ratio on the average SER of the considered regenerative system. This verifies that the SER is inversely proportional to η since for an indicative SER of 10^{-4}, an average gain of 2dB is observed when η increases from 0.1 to 0.9 for all values of μ.

Furthermore, average gains of 4dB and 1.75dB are obtained as μ increases from 0.5 to 1 and from 1 to 1.5, respectively. Likewise, Fig. 5, demonstrates the SER performance in i.n.i.d $\eta-\mu$ fading channels for 4−QAM/4−PSK constellations for the case of two relays with EPA. It is assumed that $\eta_{S,D}=0.9$, $\Omega_{S,D}=\Omega_{S,R_k}=0$dB, $\Omega_{R_k,D}=$

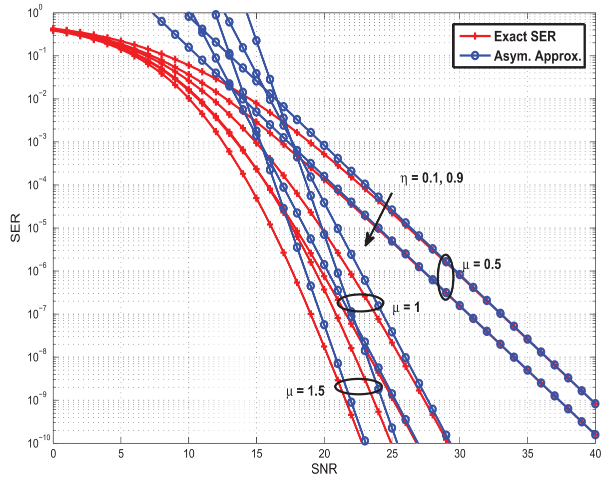

Fig. 4. SER vs average SNR with $\mu = \{0.5, 1, 1.5\}$, $\eta = \{0.1, 0.9\}$ and $\Omega_{S,D} = \Omega_{S,R_k} = \Omega_{R_k,D} = 0$ dB for 4−PSK/4−QAM, $K = 2$ and EPA.

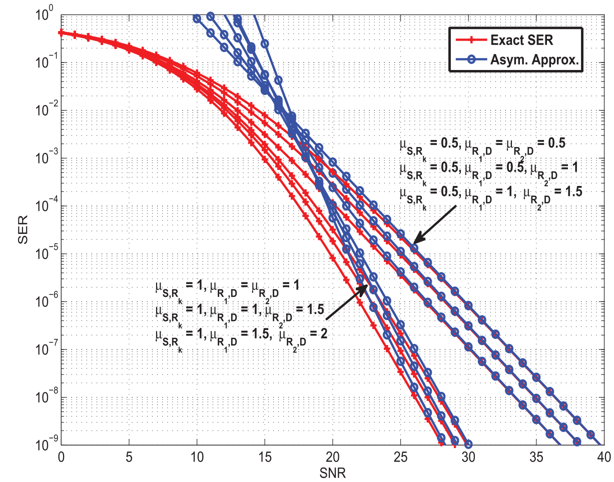

Fig. 6. SER in $\eta - \mu$ fading with $\mu_{S,D} = 0.5$ and $\eta = 0.1$, $\Omega_{S,D} = \Omega_{S,R_k} = \Omega_{R_k,D} = 0$ dB for different μ_{S,R_k} and $\mu_{R_k,D}$ for 4−QAM/4−PSK signals for $K = 2$ with EPA.

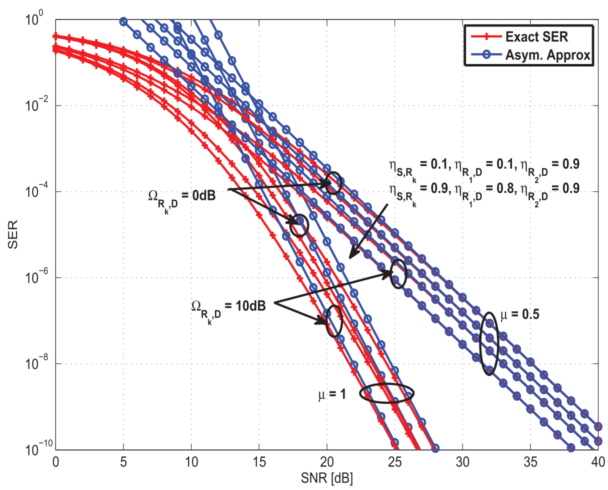

Fig. 5. SER vs SNR with $\mu = \{0.5, 1\}$, $\eta_{S,D} = 0.9$, $\Omega_{S,D} = \Omega_{S,R_k} = 0$ dB, $\Omega_{R_k,D} = \{0, 10\}$ dB with diffferent η_{S,R_k} and $\eta_{R_1,D}$ for 4−PSK/4−QAM, $K = 2$ and EPA.

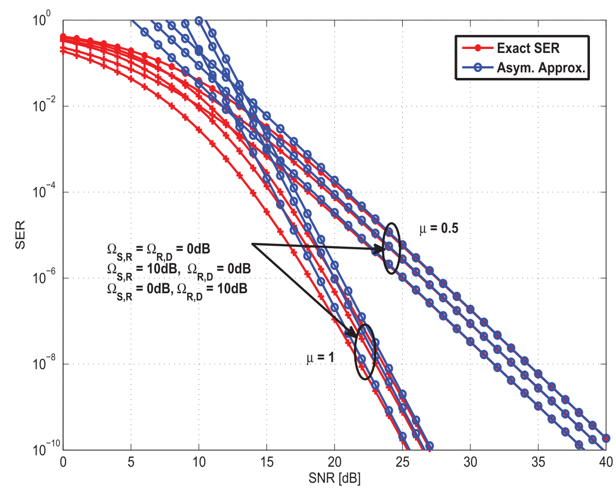

Fig. 7. SER in $\eta - \mu$ fading with $\mu = \{0.5, 1\}$, $\eta = 0.5$, and $\Omega_{S,D} = 0$ dB for different Ω_{S,R_k} and $\Omega_{R_k,D}$, 4−QAM/4−PSK, $K = 2$ and EPA.

$\{0, 10\}$dB, $\mu_{S,D} = \mu_{S,R_k} = \mu_{R_k,D} = \mu = \{0.5, 1\}$ with different values of η_{S,R_k} and $\eta_{R_1,D}$ set as $\{\eta_{S,R_k}, \eta_{R_1,D}, \eta_{R_2,D}\} = \{0.1, 0.1, 0.9\}$ and $\{0.9, 0.8, 0.9\}$, respectively. It is observed that the performance of the system improves substantially as η_{S,R_k} and $\eta_{R_1,D}$ increase as at a SER of 10^{-4} almost 1.25dB and 1.75dB gains are achieved when $\{\eta_{S,R_k}, \eta_{R_1,D}, \eta_{R_2,D}\}$ changes from $\{0.1, 0.1, 0.9\}$ to $\{0.9, 0.8, 0.9\}$ for $\Omega_{R_k,D} = \{0, 10\}$dB, for the considered values of μ.

Fig. 6 illustrates the SER performance in $\eta - \mu$ fading conditions with $\mu_{S,D} = 0.5$ and $\eta = 0.1$ for 4−QAM/4−PSK constellations and balanced links of relative channel variance 0dB for the case of two relays using EPA with different μ_{S,R_k} and non-identical values of $\mu_{R_k,D}$. The figure shows that increasing at least one of $\mu_{R_k,D}$'s value at a fixed μ_{S,R_k} or increasing both μ_{S,R_k} and $\mu_{R_k,D}$ simultaneously can improve the cooperation performance. Indicatively, at SER of 10^{-4} nearly 1.25dB and 1.75dB gains are observed when $\{\mu_{S,R_k}, \mu_{R_1}, \mu_{R_2}\}$ changes from $\{0.5, 0.5, 0.5\}$ to $\{0.5, 0.5, 1\}$ and from $\{0.5, 0.5, 1\}$ to $\{0.5, 1, 1.5\}$, respectively. Also, nearly 0.75dB and 1dB gains are achieved when $\{\mu_{R_1}, \mu_{R_2}\}$ varies from $\{1, 1\}$ to $\{1, 1.5\}$ and then to $\{1.5, 2\}$ when $\mu_{S,R_k} = 1$, whereas a gain of 4dB is shown when both μ_{S,R_k} and $\mu_{R_k,D}$ increase at the same time, for instance, from $\{0.5, 0.5, 1\}$ to $\{1, 1, 1.5\}$. Likewise, Fig. 7, depicts the SER performance for 4−QAM/4−PSK constellations for $\mu = 0.5$ and 1, $\eta = 0.5$ and unbalanced channel links employing two relays with EPA. It is shown that increasing either Ω_{S,R_k} or $\Omega_{R_k,D}$ can improve the SER and that the performance for the case of $\Omega_{S,R_k} = 0$dB and $\Omega_{R_k,D} = 10$dB is better than the reverse scenario i.e. $\Omega_{S,R_k} = 10$dB and $\Omega_{R_k,D} = 0$dB. For example, almost constant gains of 1dB and 1.75dB are achieved when $\Omega_{S,R_k} = 0$dB and $\Omega_{R_k,D} = 0$dB increase to $\Omega_{S,R_k} = 10$dB and $\Omega_{R_k,D} = 0$dB and from $\Omega_{S,R_k} = 0$dB and $\Omega_{R_k,D} = 0$dB to $\Omega_{S,R_k} = 0$dB and $\Omega_{R_k,D} = 10$dB, respectively. This verifies that in the considered regenerative protocol, the overall performance improves more when increasing average power from the relays to the destination than from the source to the relays.

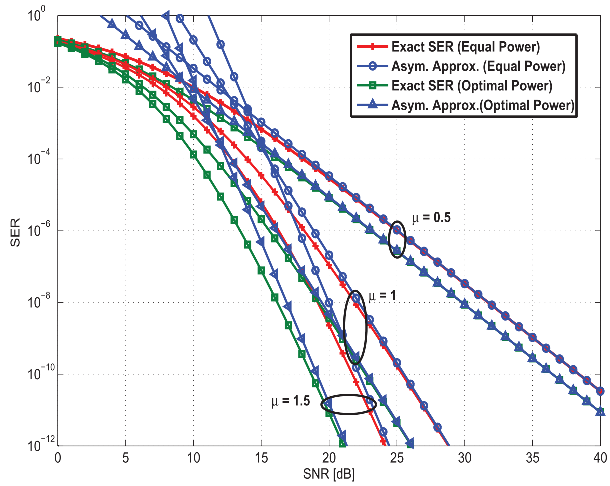

Fig. 8. SER with OPA in $\eta-\mu$ fading with $\eta=0.5$, $\Omega_{S,D}=\Omega_{S,R_k}=0$ dB and $\Omega_{R_k,D}=10$ dB for different μ and 4−QAM/4−PSK and $K=2$.

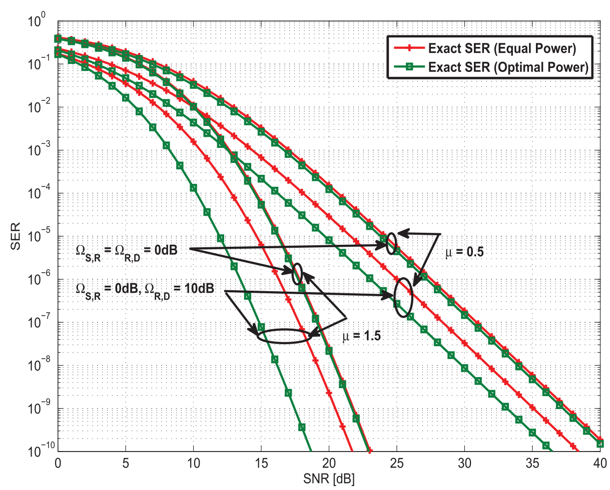

Fig. 9. SER with OPA over $\eta-\mu$ fading for $\mu_{S,D}=\mu_{S,R_k}=\mu_{R_k,D}=\mu, \eta=0.5, \Omega_{S,D}=\Omega_{S,R_k}=0$ dB with different $\Omega_{R_k,D}$ for 4−QAM/4−PSK and $K=2$.

Fig. 8, demonstrates the SER performance of the proposed OPA scheme for different values of the fading parameter μ, and assuming stronger channel variance from the relay nodes to the destination node with constant scattered-wave power ratio for the case of two relays and 4−QAM/4−PSK constellations. It is also assumed that $\mu_{S,D}=\mu_{S,R_k}=\mu_{R_k,D}=\mu$, $\Omega_{S,D}=\Omega_{S,R_k}=0$ dB, $\Omega_{R_k,D}=10$ dB and $\eta=0.5$. It is shown that when μ is small, for example $\mu=0.5$, the OPA provides small gain to the cooperation system, which, however, increases as μ increases. Indicatively, for a SER of 10^{-4} the optimal system outperforms the EPA scenario by at least 1.5dB when $\mu=0.5$ and by 2.5dB and 3dB when $\mu=1$ and $\mu=1.5$, respectively. In addition, Fig. 9 depicts the corresponding SER for the case that $\mu_{S,D}=\mu_{S,R_k}=\mu_{R_k,D}=\mu$, $\eta=0.5$, $\Omega_{S,D}=\Omega_{S,R_k}=0$dB and $\Omega_{R_k,D}=\{0,10\}$dB. It is observed that when $\Omega_{S,R_k}=\Omega_{R_k,D}=0$dB, OPA does not provide significant performance improvement for the considered DF network. On the contrary, the SER improves as the difference between Ω_{S,R_k} and $\Omega_{R_k,D}$ increases. For example, it is noticed that for a SER

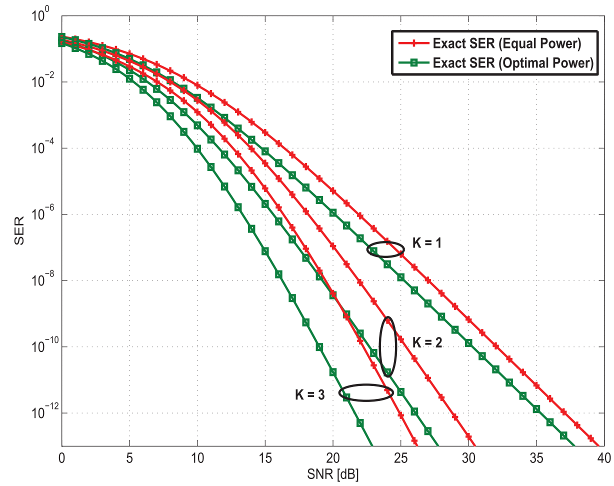

Fig. 10. SER with OPA over $\eta-\mu$ fading for $\mu=1$, $\eta=0.5$, $\Omega_{S,D}=\Omega_{S,R_k}=0$ dB and $\Omega_{R_k,D}=10$ dB for 4−PSK/4−QAM and different number of relays.

TABLE III

OPTIMAL TRANSMIT POWER ALLOCATIONS WITH DIFFERENT μ_{S,R_k} AND $\mu_{R_k,D}$ FOR $\mu_{S,D}=0.5$, $\eta=0.5$, $\Omega_{S,D}=\Omega_{S,R_k}=\Omega_{R_k,D}=0$ dB USING 4-QAM/4-PSK SIGNALS AT SNR = 20 dB

μ_{S,R_k}	$\mu_{R_k,D}$	$P_0/P \mid P_{R_1}/P$	$P_0/P \mid P_{R_1,R_2}/P$
0.5	0.5	0.6270 | 0.3730	0.4832 | 0.2584
	1	0.6572 | 0.3428	0.4914 | 0.2543
	1.5	0.6871 | 0.3129	0.5048 | 0.2476
1	0.5	0.5415 | 0.4585	0.4006 | 0.2997
	1	0.5302 | 0.4698	0.3842 | 0.3079
	1.5	0.5725 | 0.4275	0.3971 | 0.3014
1.5	0.5	0.5160 | 0.4840	0.3724 | 0.3138
	1	0.4652 | 0.5348	0.3443 | 0.3278
	1.5	0.5008 | 0.4992	0.3424 | 0.3288

TABLE IV

OPTIMAL TRANSMIT POWER ALLOCATIONS WITH DIFFERENT $\Omega_{R_k,D}$ AND $\mu_{S,D}=\mu_{S,R_k}=\mu_{R_k,D}=\mu$ FOR $\eta=0.5$, $\Omega_{S,D}=\Omega_{S,R_k}=0$ dB AND 4− QAM/4−PSK SIGNALS AT SNR = 20 dB.

μ	$\Omega_{R_k,D}$	$\frac{P_0}{P} \mid \frac{P_{R_1}}{P}$	$\frac{P_0}{P} \mid \frac{P_{R_1,R_2}}{P}$	$\frac{P_0}{P} \mid \frac{P_{R_1,R_2,R_3}}{P}$
0.5	1	0.6270 | 0.3730	0.4832 | 0.2584	0.4036 | 0.1988
	10	0.7968 | 0.2032	0.6974 | 0.1513	0.6328 | 0.1224
	100	0.9181 | 0.0819	0.8712 | 0.0644	0.8371 | 0.0543
1	1	0.5925 | 0.4075	0.4368 | 0.2816	0.3520 | 0.2160
	10	0.8316 | 0.1684	0.7343 | 0.1328	0.6658 | 0.1114
	100	0.9557 | 0.0443	0.9247 | 0.0376	0.8995 | 0.0335
1.5	1	0.5735 | 0.4265	0.4131 | 0.2935	0.3274 | 0.2242
	10	0.8496 | 0.1504	0.7549 | 0.1226	0.6850 | 0.1050
	100	0.9683 | 0.0317	0.9439 | 0.0280	0.9232 | 0.0256

of 10^{-4} and $\mu=0.5$, gains of 0.5dB and 2dB are achieved by OPA over the EPA scheme when $\Omega_{R_k,D}=\{0,10\}$dB, respectively. Similarly, gains of 0.5dB and 3dBs are obtained when μ is increased to $\mu=1.5$ while it is generally noticed that OPA is typically more effective than EPA, even in the low-SNR regime.

Fig. 10 demonstrates the SER performance of the derived OPA and EPA scenarios for single, two and three relays over symmetric $\eta-\mu$ fading scenario, i.e., with constant μ and constant scattered-power ratios η and unbalanced channel variances from source-to-relay and from relay-to-destination. It is assumed that $\mu_{S,D}=\mu_{S,R_k}=\mu_{R_k,D}=1$, $\eta=0.5$, whereas $\Omega_{S,D}=\Omega_{S,R_k}=0$dB and $\Omega_{R_k,D}=10$dB. It is shown that the OPA strategy clearly outperforms its EPA counterpart since the gain for a SER of 10^{-4} is 2dB, 2.5dB and 2.75dB for one, two and three relays, respectively. The characteristics of the OPA strategy are further analyzed with the aid

TABLE V
OPTIMAL TRANSMIT POWER ALLOCATIONS WITH DIFFERENT MODULATIONS AND $\mu_{S,D} = \mu_{S,R_k} = \mu_{R_k,D} = \mu$, $\eta = 0.5$, $\Omega_{S,D} = \Omega_{S,R_k} = \Omega_{R_k,D} = 0$ dB FOR TWO RELAYS AT SNR = 20 dB.

	$4-PSK$	$16-PSK$	$16-QAM$
μ	$P_0/P \mid P_{R_1,R_2}/P$	$P_0/P \mid P_{R_1,R_2}/P$	$P_0/P \mid P_{R_1,R_2}/P$
0.5	0.4832 | 0.2584	0.4932 | 0.2534	0.5113 | 0.2443
1	0.4368 | 0.2816	0.4392 | 0.2804	0.4572 | 0.2714
1.5	0.4130 | 0.2935	0.4138 | 0.2931	0.4287 | 0.2857

of Tables III, IV and V, which depict the optimal power ratios allocated to the source and the relay-nodes in terms of P_0/P and P_{R_k}/P, which are evaluated numerically. In case of multiple relays, the relays are assigned with equal powers i.e. $P_{R_k}/P = P_{R_{k+1}}/P$. The power ratios allocated to the source and relay nodes for asymmetric and balanced channel conditions are tabulated indicating that the numerical values are in tight agreement with the formulated power strategy in Section IV. Table IV also corresponds to the case that the source is assigned with high proportion of power when $\Omega_{R_k,D}$ is larger than Ω_{S,R_k}, i.e., unbalanced channel links, whereas Table V verifies that the optimal power allocation scheme is dependent upon the considered modulation scheme.

VI. CONCLUSION

In this paper, we analyzed the end-to-end performance and optimum power allocation of regenerative cooperative systems over generalized fading channels. Novel exact and asymptotic expressions for the end-to-end SER assuming $M-$PSK and $M-$QAM modulated signals were derived over independent and identically distributed as well as independent and non-identically distributed $\eta - \mu$ fading channels. The derived analytic expressions were then utilized to draw insights of the different fading parameters of the model in the corresponding generalized fading conditions and their impact on the end-to-end system performance. The offered results were subsequently employed in developing an asymptotically optimum power allocation scheme, under a total sum-power constraint, which was shown to outperform significantly conventional equal power allocation strategy. It was also shown that the optimum power allocation scheme is practically independent of the scattered-waves power ratio parameter from source-to-destination, while it is dependent upon the number of multipath clusters as well as the selected modulation scheme and that it overall provides significant performance enhancement.

APPENDIX I
A MATLAB ALGORITHM FOR COMPUTING THE GENERALIZED LAURICELLA FUNCTION

The Generalized Lauricella function is defined by the following non-infinite single integral,

$$F_D^{(n)}(\mathrm{a}, b_1, \cdots, b_n; c; x_1, \cdots, x_n) \triangleq \times \frac{\Gamma(c)}{\Gamma(\mathrm{a})\Gamma(c-\mathrm{a})} \int_0^1 t^{\mathrm{a}-1} \frac{(1-t)^{c-\mathrm{a}-1}}{(1-x_1 t)^{b_1} \cdots (1-x_n t)^{b_n}} \mathrm{d}t \tag{108}$$

The numerical evaluation of the above representation was also discussed in [58, Appendix E] and can be straightforwardly evaluated with the aid of the proposed MATLAB algorithm as

```
Function FD = Lauricella(a, b1, ··· , bn, c, x1, ··· , xn);
f = gamma (c)./(gamma (a). ∗ gamma (c − a));
Q = @(t) f. ∗ t.^(a − 1). ∗ (1 − t).^(c − a − 1). ∗ ···
(1 − x1. ∗ t).^(−b1) ··· (1 − xn. ∗ t).^(−bn);
FD = quad(Q, 0, 1)
```

APPENDIX II
PROOF OF CONVEXITY OF THE OPTIMIZATION PROBLEM

We provide the proof for the convexity of the SER expression by using (76). For mathematical tractability, we consider the proof for three relay-nodes. Based on this, the proof for larger number of nodes scenario follows immediately. To this end, the asymptotic SER can be expressed as

$$\begin{aligned} P_{\mathrm{SER}}^D \approx & \frac{K_1}{a_0^{2(\mu_{S,D}+\mu_{S,R_1}+\mu_{S,R_2}+\mu_{S,R_3})}} \\ & + \frac{K_2}{a_0^{2(\mu_{S,D}+\mu_{S,R_1}+\mu_{S,R_2})} a_{R_3}^{2\mu_{R_3,D}}} \\ & + \frac{K_3}{a_0^{2(\mu_{S,D}+\mu_{S,R_1}+\mu_{S,R_3})} a_{R_2}^{2\mu_{R_2,D}}} \\ & + \frac{K_4}{a_0^{2(\mu_{S,D}+\mu_{S,R_1})} a_{R_2}^{2\mu_{R_2,D}} a_{R_3}^{2\mu_{R_3,D}}} \\ & + \frac{K_5}{a_0^{2(\mu_{S,D}+\mu_{S,R_2}+\mu_{S,R_3})} a_{R_1}^{2\mu_{R_1,D}}} \\ & + \frac{K_6}{a_0^{2(\mu_{S,D}+\mu_{S,R_2})} a_{R_1}^{2\mu_{R_1,D}} a_{R_3}^{2\mu_{R_3,D}}} \\ & + \frac{K_7}{a_0^{2(\mu_{S,D}+\mu_{S,R_3})} a_{R_1}^{2\mu_{R_1,D}} a_{R_2}^{2\mu_{R_2,D}}} \\ & + \frac{K_8}{a_0^{2\mu_{S,D}} a_{R_1}^{2\mu_{R_1,D}} a_{R_2}^{2\mu_{R_2,D}} a_{R_3}^{2\mu_{R_3,D}}} \end{aligned} \tag{109}$$

where $K_1, \cdots, K_8$ are related to the channel parameters. Let $f_1(a_0, \cdots, a_{R_3}), \cdots, f_8(a_0, \cdots, a_{R_3})$ be functions which represent each term of P_{SER}^D. For example, we assign (110), shown at the bottom of the next page. The second order derivative of $f_1(a_0)$ w.r.t a_0 is given by

$$\begin{aligned} \frac{\partial^2 f_1(a_0)}{\partial^2 a_0} = & \frac{4K_1(\mu_{S,D}+\mu_{S,R_1}+\mu_{S,R_2}+\mu_{S,R_3})}{a_0^{2(\mu_{S,D}+\mu_{S,R_1}+\mu_{S,R_2}+\mu_{S,R_3}+1)}} \\ & \times \left(\mu_{S,D}+\mu_{S,R_1}+\mu_{S,R_2}+\mu_{S,R_3}+\frac{1}{2}\right). \end{aligned} \tag{111}$$

The Hessian matrix of $f_2(a_0, a_{R_3})$, $\bigtriangledown^2 f_2(a_0, a_{R_3})$, can be determined by (112), at the bottom of the this page. The principal minors of the matrix $H(a_0, a_{R_3})$, $H_{11}(a_0, a_{R_3}) \geq 0$, $H_{22}(a_0, a_{R_3}) \geq 0$ and $H_{11}H_{22} \geq H_{12}H_{21}$. To this effect, the symmetric Hessian matrix $H(a_0, a_{R_3})$ is positive semi-definite (PSD). Given that

$$\frac{\partial^2 f_1(a_0)}{\partial^2 a_0} \geq 0 \tag{113}$$

and $H(a_0, a_{R_3})$ is PSD, i.e.,

$$\bigtriangledown^2 f_2(a_0, a_{R_3}) \succeq 0 \tag{114}$$

it follows by the second order test in [57] that both $f_1(a_0)$ and $f_2(a_0, a_{R_3})$ functions are convex. Following the same methodology, it is shown that the functions $f_3, \cdots, f_8$ are also convex. Hence, by the sum rule of convexity [57, Section (3.2.1)] it follows that the total function P_{SER}^D is convex w.r.t a_0, a_{R_1}, a_{R_2} and a_{R_3}.

Acknowledgment

The authors would like to thank the editor and the anonymous reviewers for their constructive comments and criticism.

References

[1] J. N. Laneman and G. W. Wornell, "Distributed space-time coded protocols for exploiting cooperative diversity in wireless networks," *IEEE Trans. Inf. Theory*, vol. 49, no. 10, pp. 2415–2425, Nov. 2003.

[2] J. Boyer, D. D. Falconer, and H. Yanikomeroglu, "Multihop diversity in wireless relaying channels," *IEEE Trans. Commun.*, vol. 52, no. 10, pp. 1820–1830, Oct. 2004.

[3] A. Nosratinia, T. E. Hunter, and A. Hedayat, "Cooperative communication in wireless networks," *IEEE Commun. Mag.*, vol. 42, no. 10, pp. 74–80, Oct. 2004.

[4] Y. Zou, B. Zheng, and J. Zhu, "Outage analysis of opportunistic cooperation over Rayleigh fading channels," *IEEE Trans. Wireless Commun.*, vol. 8, no. 6, pp. 3077–3085, Jun. 2009.

[5] M. Di Renzo, F. Graziosi, and F. Santucci, "A unified framework for performance analysis of CSI-assisted cooperative communications over fading channels," *IEEE Trans. Commun.*, vol. 57, no. 9, pp. 2551–2557, Sep. 2009.

[6] Y. Zou, B. Zheng, and W. P. Zhu, "An opportunistic cooperation scheme and its BER analysis," *IEEE Trans. Wireless Commun.*, vol. 8, no. 9, pp. 4492–4497, Sep. 2009.

[7] Z. Zhao, M. Peng, Z. Ding, W. Wang, and H. H. Chen, "Denoise-and-forward network coding for two-way relay MIMO systems," *IEEE Trans. Veh. Technol.*, vol. 63, no. 2, pp. 775–788, Feb. 2014.

[8] C. Zhong, H. A. Suraweera, G. Zheng, I. Krikidis, and Z. Zhang, "Wireless information and power transfer with full duplex relaying," *IEEE Trans. Commun.*, vol. 62, no. 10, pp. 3447–3461, Oct. 2014.

[9] Z. Ding, I. Krikidis, B. Sharif, and H. V. Poor, "Wireless information and power transfer in cooperative networks with spatially random relays," *IEEE Trans. Wireless Commun.*, vol. 13, no. 8, pp. 4440–4453, Aug. 2014.

[10] J. N. Laneman, D. N. C. Tse, and G. W. Wornell, "Cooperative diversity in wireless networks: Efficient protocols and outage behavior," *IEEE Trans. Inf. Theory*, vol. 50, no. 12, pp. 3062–3080, Dec. 2004.

[11] J. Yang, P. Fan, and Z. Ding, "Capacity of AF two-way relaying with multiuser scheduling in Nakagami–*m* fading communications," *IET Elect. Lett.*, vol. 48, no. 22, pp. 1432–1434, Oct. 2012.

[12] V. Asghari, D. B. da Costa, and S. Aissa, "Performance analysis for multihop relaying channels with Nakagami–*m* fading: Ergodic capacity upper-bounds and outage probability," *IEEE Trans. Commun.*, vol. 60, no. 10, pp. 2761–2767, Oct. 2012.

[13] Z. Ding and H. V. Poor, "Cooperative Energy Harvesting Networks with Spatially Random Users," *IEEE Signal Process. Lett.*, vol. 20, no. 12, pp. 1211–1214, Dec. 2013.

[14] M. Elkashlan, P. L. Yeoh, N. Yang, T. Q. Duong, and C. Leung, "A comparison of two MIMO relaying protocols in Nakagami–*m* fading," *IEEE Trans. Veh. Technol.*, vol. 61, no. 3, pp. 1416–1422, Mar. 2012.

[15] Z. Ding, S. Perlaza, I. Esnaola, and H. V. Poor, "Power Allocation Strategies in Energy Harvesting Wireless Cooperative Networks," *IEEE Trans. Wireless Commun.*, vol. 13, no. 2, pp. 846–860, Feb. 2014.

[16] P. L. Yeoh, M. Elkashlan, Z. Chen, and I. B. Collings, "SER of multiple amplify-and-forward relays with selection diversity," *IEEE Trans. Commun.*, vol. 59, no. 8, pp. 2078–2083, Aug. 2011.

[17] G. Zhu, C. Zhong, H. A. Suraweera, Z. Zhang, C. Yuen, and R. Yin, "Ergodic capacity comparison of different relay precoding schemes in dual-hop AF systems with co-channel interference," *IEEE Trans. Commun.*, vol. 62, no. 7, pp. 2314–2328, Jul. 2014.

[18] S.-Q. Huang, H.-H. Chen, and M.-Y. Lee, "Performance bounds of multi-relay decode-and-forward cooperative networks over Nakagami–*m* fading channels," in *Proc. IEEE Int. Conf. Commun.*, Kyoto, Japan, Jun. 5–9, 2011, pp. 1–5.

[19] T. Duong, V. N. Q. Bao, and H. J. Zepernick, "On the performance of selection decode-and-forward relay networks over Nakagami–*m* fading channels," *IEEE Commun. Lett.*, vol. 13, no. 3, pp. 172–174, Mar. 2009.

[20] S. N. Datta, S. Chakrabarti, and R. Roy, "Comprehensive error analysis of multi-antenna decode-and-forward relay in fading channels," *IEEE Commun. Lett.*, vol. 16, no. 1, pp. 47–49, Jan. 2012.

[21] S. N. Datta and S. Chakrabarti, "Unified error analysis of dual-hop relay link in Nakagami–*m* fading channels," *IEEE Commun. Lett.*, vol. 14, no. 10, pp. 897–899, Oct. 2010.

[22] S. S. Ikki and M. H. Ahmed, "Multi-branch decode-and-forward cooperative diversity networks performance analysis over Nakagami–*m* fading channels," *IET Commun.*, vol. 5, no. 6, pp. 872–878, Jun. 2011.

[23] S. S. Ikki and M. H. Ahmed, "Performance analysis of adaptive decode-and-forward cooperative diversity networks with best-relay selection," *IEEE Trans. Commun.*, vol. 58, no. 1, pp. 68–72, Jan. 2010.

[24] K. J. Kim, T. Q. Duong, H. V. Poor, and M. H. Lee, "Performance analysis of adaptive decode-and-forward cooperative single-carrier systems," *IEEE Trans. Veh. Technol.*, vol. 61, no. 7, pp. 3332–3337, Jul. 2012.

[25] M. K. Fikadu, P. C. Sofotasios, Q. Cui, G. K. Karagiannidis, and M. Valkama, "Exact error analysis and energy-efficiency optimization of regenerative relay systems," *IEEE Trans. Veh. Technol.*, 2015, submitted for publication.

[26] Y. Lee and M.-H. Tsai, "Performance of decode-and-forward cooperative communications over Nakagami–*m* fading channels," *IEEE Trans. Veh. Technol.*, vol. 58, no. 3, pp. 1218–1228, Mar. 2009.

[27] Y.-R. Tsai and L.-C. Lin, "Optimal power allocation for decode-and forward cooperative diversity under an outage performance constraint," *IEEE Commun. Lett.*, vol. 14, no. 10, pp. 945–947, Oct. 2010.

[28] A. K. Sadek, W. Su, and K. J. Ray Liu, "Multi-node cooperative communications in wireless networks," *IEEE Trans. Signal Process.*, vol. 55, no. 1, pp. 341–355, Jan. 2007.

$$f_1(a_0) = \frac{K_1}{a_0^{2(\mu_{S,D}+\mu_{S,R_1}+\mu_{S,R_2}+\mu_{S,R_3})}}, \; f_2(a_0, a_{R_3}) = \frac{K_2}{a_0^{2(\mu_{S,D}+\mu_{S,R_1}+\mu_{S,R_2})} a_{R_3}^{2\mu_{R_3,D}}}, \cdots \tag{110}$$

$$H(a_0, a_{R_3}) = \begin{bmatrix} \frac{4K_2(\mu_{S,D}+\mu_{S,R_1}+\mu_{S,R_2})(\mu_{S,D}+\mu_{S,R_1}+\mu_{S,R_2}+\frac{1}{2})}{a_0^{2(\mu_{S,D}+\mu_{S,R_1}+\mu_{S,R_2}+1)} a_{R_3}^{2\mu_{R_3,D}}} & \frac{4K_2\mu_{R_3,D}(\mu_{S,D}+\mu_{S,R_1}+\mu_{S,R_2})}{a_0^{2(\mu_{S,D}+\mu_{S,R_1}+\mu_{S,R_2}+\frac{1}{2})} a_{R_3}^{2\mu_{R_3,D}+1}} \\ \frac{4K_2\mu_{R_3,D}(\mu_{S,D}+\mu_{S,R_1}+\mu_{S,R_2})}{a_0^{2(\mu_{S,D}+\mu_{S,R_1}+\mu_{S,R_2}+\frac{1}{2})} a_{R_3}^{2\mu_{R_3,D}+1}} & \frac{4K_2\mu_{R_3,D}(\mu_{R_3,D}+\frac{1}{2})}{a_0^{2(\mu_{S,D}+\mu_{S,R_1}+\mu_{S,R_2})} a_{R_3}^{2(\mu_{R_3,D}+1)}} \end{bmatrix} \tag{112}$$

[29] Y.-W. Hong, W.-J. Huang, F.-H. Chiu, and C.-C. J. Kuo, "Cooperative communications in resource-constrained wireless networks," *IEEE Signal Process. Mag.*, vol. 24, no. 3, pp. 47–57, May 2007.
[30] Y. Lee, M.-H. Tsai, and S.-I. Sou, "Performance of decode-and-forward cooperative communications with multi dual-hop relays over Nakagami–*m* fading channels," *IEEE Trans. Wireless Commun.*, vol. 8, no. 6, pp. 2853–2859, Jun. 2009.
[31] W. Braun and U. Dersch, "A physical mobile radio channel model," *IEEE Trans. Veh. Technol.*, vol. 40, no. 2, pp. 472–482, May 1991.
[32] M. D. Yacoub, "The κ–μ distribution and the η–μ distribution," *IEEE Antennas Propag. Mag.*, vol. 49, no. 1, pp. 68–81, Feb. 2007.
[33] P. C. Sofotasios, T. A. Tsiftsis, Y. A. Brychkov, S. Freear, M. Valkama, and G. K. Karagiannidis, "Analytic expressions and bounds for special functions and applications in communication theory," *IEEE Trans. Inf. Theory*, vol. 60, no. 12, pp. 7798–7823, Dec. 2014.
[34] P. C. Sofotasios, S. Muhaidat, M. Valkama, M. Ghogho, and G. K. Karagiannidis, "Entropy and channel capacity under optimum power and rate adaptation over generalized fading conditions," *IEEE Signal Process. Lett.*, vol. 22, no. 11, pp. 2162–2166, Nov. 2015.
[35] S. Ki Yoo, P. C. Sofotasios, S. L. Cotton, M. Matthaiou, M. Valkama, and G. K. Karagiannidis, "The η–μ / inverse gamma composite fading model," in *Proc. IEEE 26th Int. Symp. Pers. Indoor Mobile Radio Commun. (PIMRC'15)*, Aug./Sep. 2015
[36] A. Bagheri, P. C. Sofotasios, T. A. Tsiftsis, A. Shahzadi, and M. Valkama, "AUC study of energy detection based spectrum sensing over η–μ and α–μ fading channels," *Proc. IEEE Int. Conf. Commun. (ICC'15)*, Jun. 2015, pp. 1410–1415.
[37] P. C. Sofotasios, M. K. Fikadu, K. Ho-Van, M. Valkama, and G. K. Karagiannidis, "The area under a receiver operating characteristic curve over enriched multipath fading conditions," in *Proc. IEEE Globecom*, Austin, TX, USA, Dec. 2014, pp. 3490–3495.
[38] P. C. Sofotasios, M. Valkama, Y. A. Brychkov, T. A. Tsiftsis, S. Freear, and G. K. Karagiannidis, "Analytic solutions to a Marcum *Q*–function-based integral and application in energy detection," in *Proc. CROWNCOM*, Oulu, Finland, Jun. 2014
[39] P. C. Sofotasios, T. A. Tsiftsis, M. Ghogho, L. R. Wilhelmsson, and M. Valkama, "The η–μ/inverse Gaussian distribution: A novel physical multipath/shadowing fading model," in *Proc. IEEE Int. Conf. Commun.*, Budapest, Hungary, Jun. 2013, pp. 5715–5719.
[40] J. C. Silveira Santos Filho, and M. D. Yacoub, "Highly accurate η–μ approximation to sum of *M* independent non-identical Hoyt variates," *IEEE Antennas Wireless Propag. Lett.*, vol. 4, no. 1, pp. 436–438, Dec. 2005.
[41] P. C. Sofotasios and S. Freear, "The η–μ/gamma and the λ–μ/gamma multipath/shadowing distributions," in *Proc. Aust. Telecommun. Netw. Appl. Conf. (ATNAC'11)*, Melbourne, VIC, Australia, Nov. 2011
[42] P. C. Sofotasios and S. Freear, "The η–μ/gamma composite fading model," in *Proc. IEEE Int. Conf. Wireless Inf. Technol. Syst. (ICWITS '10)*, Honolulu, HI, USA, Aug/Sep. 2010
[43] D. B. da Costa and M. D. Yacoub, "Accurate approximations to the sum of generalized random variables and applications in the performance analysis of diversity systems," *IEEE Trans. Commun.*, vol. 57, no. 5, pp. 1271–1274, May 2009.
[44] K. Peppas, F. Lazarakis, A. Alexandridis, and K. Dangakis, "Error performance of digital modulation schemes with MRC diversity reception over η–μ fading channels," *IEEE Trans. Wireless Commun.*, vol. 8, no. 10, pp. 4974–4980, Oct. 2009.
[45] H. Yu, G. Wei, F. Ji, and X. Zhang, "On the error probability of cross–QAM with MRC reception over generalized η–μ fading channels," *IEEE Trans. Veh. Technol.*, vol. 60, no. 6, pp. 2631–2643 Jul. 2011.
[46] V. Asghari, D. B. Costa, and S. Aissa, "Symbol error probability of rectangular QAM in MRC systems with correlated η–μ fading channels," *IEEE Trans. Veh. Technol.*, vol. 59, no. 3, pp. 1497–1503, Mar. 2010.
[47] D. M. Jimenez and J. F. Paris, "Outage probability analysis for η–μ fading channels," *IEEE Commun. Lett.*, vol. 14, no. 6, pp. 521–523, Jun. 2010.
[48] N. Y. Ermolova, "Moment generating functions of the generalized η–μ and κ–μ distributions and their applications to performance evaluations of communication systems," *IEEE Commun. Lett.*, vol. 12, no. 7, pp. 502–504, Jul. 2008.
[49] W.-G. Li, H.-M. Chen, and M. Chen, "Outage probability of dual-hop decode-and-forward relaying systems over generalized fading channels," *Eur. Trans. Telecommun.*, vol. 21, no. 1, pp. 86–89, Jan. 2010.
[50] M. O. Hasna and M.-S. Alouini, "Optimal power allocation for relayed transmissions over Rayleigh-fading channels," *IEEE Trans. Wireless Commun.*, vol. 3, no. 6, pp. 1999–2004, Nov. 2004.
[51] I. S. Gradshteyn and I. M. Ryzhik, *Tables of Integrals, Series, and Products*, 7th ed. New York, NY, USA: Academic, 2007.
[52] M. K. Simon and M.-S. Alouni, *Digital Communication Over Fading Channels*, 2nd ed. Hoboken, NJ, USA: Wiley, 2005.
[53] G. P. Efthymoglou, T. Piboongungon, and V. A. Aalo, "Error rates of M-ary signals with multichannel reception in Nakagami–m fading channels," *IEEE Commun. Lett.*, vol. 10, no. 2, pp. 100–102, Feb. 2006.
[54] S. Amara, H. Boujemaa, and N. Hamdi, "SEP of cooperative systems using amplify and forward or decode and forward relaying over Nakagami–m fading channels," in *Proc. IEEE Int. Conf. Circuits Syst.*, Nov. 6–8, 2009, pp. 1–5.
[55] N. Y. Ermolova, "Useful integrals for performance evaluation of communication systems in generalized η–μ and κ–μ fading channels," *IET Commun.*, vol. 3, no. 2, pp. 303–308, Feb. 2009.
[56] A. P. Prudnikov, Y. A. Brychkov, and O. I. Marichev, *Integrals and Series Volume 3: More Special Functions*, 1st ed. New York, NY, USA: Gordon and Breach, 1986.
[57] S. Boyd and L. Vandenberghe, *Convex Optimization*. Cambridge, U.K.: Cambridge Univ. Press, 1994.
[58] J. F. Paris, "Statistical characterization of κ–μ shadowed fading," *IEEE Trans. Veh. Technol.*, vol. 63, no. 2, pp. 518–526, Feb. 2014.

Mulugeta K. Fikadu received the M.Sc. degree in communication engineering from the Department of Electrical and Computer Engineering, Addis Ababa University, Addis Ababa, Ethiopia, in 2007. He is currently pursuing the doctoral degree at the Department of Electronics and Communications Engineering, Tampere University of Technology (TUT), Tampere, Finland, where he is working as a Project Researcher. He has also worked as a Project Researcher with the Department of Computer Science, Communications and Systems Engineering Group, University of Vaasa, Vaasa, Finland, in 2011. His research interests include resource allocation in wireless cooperative networks, space-time coding, and MIMO-OFDM systems.

Paschalis C. Sofotasios (S'09–M'11) was born in Volos, Greece, in 1978. He received the M.Eng. degree from University of Newcastle, Newcastle upon Tyne, U.K., the M.Sc. degree from the University of Surrey, Guildford, U.K., and the Ph.D. degree from the University of Leeds, Leeds, U.K., in 2004, 2006, and 2011, respectively. His master's studies were funded by a scholarship from UK-EPSRC and his doctoral studies were sponsored by UK-EPSRC and Pace plc. He was a Postdoctoral Researcher with the University of Leeds until August 2013 and a Visiting Researcher at the University of California, Los Angleles, CA, USA, Aristotle University of Thessaloniki, Thessaloniki, Greece, and Tampere University of Technology, Tampere, Finland. Since Fall 2013, he has been a Postdoctoral Research Fellow with the Department of Electronics and Communications Engineering, Tampere University of Technology, and also with the Wireless Communications Systems Group, Aristotle University of Thessalonki. His research interests include fading channel characterization, cognitive radio, cooperative communications, optical wireless communications as well as in the theory and properties of special functions and statistical distributions. He was the recipient of the 2012 and 2015, 2016 Exemplary Reviewer Award by the IEEE COMMUNICATION LETTERS and IEEE TRANSACTIONS ON COMMUNICATIONS, respectively. He was also the recipient of the BEST PAPER AWARD at the ICUFN '13.

Sami Muhaidat (M'08–SM'11) received the Ph.D. degree in electrical and computer engineering from the University of Waterloo, Waterloo, ON, Canada, in 2006. From 2007 to 2008, he was an NSERC Postdoctoral Fellow with the Department of Electrical and Computer Engineering, University of Toronto, ON, Canada. From 2008 to 2012, he was an Assistant Professor with the School of Engineering Science, Simon Fraser University, Burnaby, BC, Canada. He is currently an Associate Professor with Khalifa University, Abu Dhabi, UAE, and a Visiting Professor at the Department of Electrical and Computer Engineering, University of Western Ontario, London, ON, Canada. He is also a Visiting

Reader at the Faculty of Engineering, University of Surrey, Surrey, U.K. His research interests include advanced digital signal processing techniques for communications, cooperative communications, vehicular communications, MIMO, and machine learning. He has authored more than 100 journal and conference papers on these topics. He currently serves as a Senior Editor for the IEEE COMMUNICATIONS LETTERS, an Editor for the IEEE TRANSACTIONS ON COMMUNICATIONS, and an Associate Editor for the IEEE TRANSACTIONS ON VEHICULAR TECHNOLOGY. He was the recipient of several scholarships during his undergraduate and graduate studies. He was also a winner of the 2006 NSERC postdoctoral fellowship competition.

Qimei Cui (M'09–SM'15) received the B.E. and M.S. degrees in electronic engineering from Hunan University, Changsha, China, in 2000 and 2003, the Ph.D. degree in telecommunications from Beijing University of Posts and Telecommunications (BUPT), Beijing, China, in 2006. She is currently a Full Professor in the School of Information and Communication Engineering (SICE), BUPT. Her research interests include transmission theory and networking technology for next generation broadband wireless communications and green communications. She was the recipient of the only Best Paper Award at IEEE ISCIT 2012, Best Paper Award in IEEE WCNC 2014, the Honorable Mention Demo Award at ACM MobiCom 2009, and the Young Scientist Award at URSI GASS 2014 etc.

George K. Karagiannidis (M'96–SM'03–F'14) was born in Pithagorion, Samos Island, Greece. He received the University Diploma (5 years) and Ph.D. degrees in electrical and computer engineering from the University of Patras, Patron, Greece, in 1987 and 1999, respectively. From 2000 to 2004, he was a Senior Researcher with the Institute for Space Applications and Remote Sensing, National Observatory of Athens, Athens, Greece. In June 2004, he joined the faculty of Aristotle University of Thessaloniki, Thessaloniki, Greece, where he is currently a Professor with the Department of Electrical and Computer Engineering and the Director of Digital Telecommunications Systems and Networks Laboratory. His research interests include digital communications systems with emphasis on wireless communications, optical wireless communications, wireless power transfer and applications, molecular communications, communications and robotics, and wireless security. He is a Honorary Professor with the South West Jiaotong University, Chengdu, China.

He is the author or coauthor of more than 400 technical papers published in scientific journals and presented at international conferences. He is also the author of the Greek edition of the book *Telecommunications Systems* and the coauthor of the book *Advanced Optical Wireless Communications Systems* (Cambridge Publications, 2012).

Dr. Karagiannidis has been involved as the General Chair, the Technical Program Chair, and a member of Technical Program Committees in several IEEE and non-IEEE conferences. Previously, he was an Editor of the IEEE TRANSACTIONS ON COMMUNICATIONS, a Senior Editor of the IEEE COMMUNICATIONS LETTERS, an Editor of the *EURASIP Journal of Wireless Communications and Networks*, and several times as a Guest Editor of IEEE SELECTED AREAS IN COMMUNICATIONS. From 2012 to 2015, he was the Editor-in Chief of the IEEE COMMUNICATIONS LETTERS. He has been selected as a 2015 Thomson Reuters Highly Cited Researcher.

Mikko Valkama (S'00–M'01–SM'15) was born in Pirkkala, Finland, on November 27, 1975. He received the M.Sc. and Ph.D. degrees (with Hons.) in electrical engineering from Tampere University of Technology (TUT), Tampere, Finland, in 2000 and 2001, respectively. In 2003, he was working as a Visiting Researcher with the Communications Systems and Signal Processing Institute, San Diego State University, San Diego, CA, USA. Currently, he is a Full Professor and the Department Vice-Head of the Department of Electronics and Communications Engineering, TUT. His research interests include communications signal processing, estimation and detection techniques, signal processing algorithms for software-defined flexible radios, cognitive radio, full-duplex radio, radio localization, 5G mobile cellular radio, digital transmission techniques such as different variants of multicarrier modulation methods and OFDM, and radio resource management for ad-hoc and mobile networks. In 2002, He was the recipient of the Best Ph.D. Thesis Award from the Finnish Academy of Science and Letters for his dissertation entitled ”Advanced I/Q signal processing for wideband receivers: Models and algorithms.”